

GEOTECHNICAL RESEARCH CENTRE

**RECENT STUDIES ON WHEEL
AND TRACK-SOIL INTERACTION
AND VANE-CONE PREDICTION**

BY

RAYMOND N. YONG

&

VEHICLE MOBILITY LABORATORY STAFF

SOIL MECHANICS SERIES NO. 39

MAY 1978



**McGill University
Montreal, Que Canada**

**Report to:
Defence Research
Establishment Ottawa**

**Department of Supply and Services
Contract No. 068U CD 3237007/8
Serial No. 35U77-00087/65**

ISBN 0541-6329

TAZIO,5
85

FOREWORD -

The problem of wheel and track soil interaction has been covered most recently and summarized insofar as McGill Vehicle Mobility Laboratory work for the 1977-1978 research year is concerned, in the two papers presented herein. These have been written for -

*The Sixth International Conference of the
International Society for Terrain-Vehicle Systems,
Vienna, August 1978.*

and are published in the Proceedings of the Conference.

APPLICATION OF VANE-CONE TESTS ON SOIL FOR
DETERMINATION OF TRAFFICABILITY

by

R. N. Yong and A. F. Youssef

prepared for

SIXTH INTERNATIONAL CONFERENCE

I.S.T.V.S.

Vienna

August 1978

APPLICATION OF VANE-CONE TESTS ON SOIL FOR
DETERMINATION OF TRAFFICABILITY

by

R. N. Yong¹ and A. F. Youssef²

ABSTRACT

In the assessment of trafficability of a particular soil the need to distinguish between the ability of the material to provide flotation or traction thrust capability is apparent. Since flotation capability refers primarily to the ability of the material to support the applied vehicle load, thrust development which depends on interactions at the surface is not easily assessed. Hence, it becomes important to provide a means for obtaining information of the soil or snow material which could lead to analysis for shear and thrust interaction at the vehicle-ground interface.

This study provides measurements obtained with a vane-cone device on soil where analyses lead to the procurement of both deformation and shear-slip energy expenditures. In comparing the predictive capability using the associated analysis from vane-cone measurements and other available techniques, the results show that the utilisation of data in terms of *energetics* provides for a method of analysis and prediction which responds more closely to the problem at hand.

¹ William Scott Professor of Civil Engineering and Applied Mechanics, and Director, Geotechnical Research Centre, McGill University, Montreal, Canada.

² Research Associate, Geotechnical Research Centre, McGill University, Montreal, Canada.

INTRODUCTION

Interaction between vehicle and terrain is achieved through the running gear system which is either a wheel system or a track/device, or some other equivalent system. The mechanics of interaction between wheel-soil and track-soil have been developed previously in many published reports by Yong. The essential items for the interaction between these running gears and the terrain are summarized in Figs. 1 and 2.

Note that for optimum mobility purposes, it is desirable that the vehicle be able to move from one point to another specified position with the least amount of wasted motion. To achieve this, the vehicle must not only be supported by the terrain, in addition, the terrain must provide sufficient resistance [capability] wherein thrust can be developed between the running gear and the terrain itself with minimal slip loss. Immobilization therefore can arise as a result of lack of ground support or lack of strength in the terrain to provide the wherewithal for development of thrust. These are demonstrated as sinkage immobilization, or slip immobilization. There are obviously combinations between the two which may provide for immobilization through interaction between these two primary mechanizations.

In the assessment of trafficability of a particular soil the need to distinguish between the ability of the material to provide flotation or traction thrust capability is apparent. Since flotation capability refers primarily to the ability of the material to support the applied vehicle load, thrust development which depends on interactions at the surface is not easily assessed. Hence, it becomes important to provide a means for obtaining information of the soil or snow material

which could lead to analysis for shear and thrust interaction at the vehicle-ground interface.

In order that one might predict the behaviour of a system, it is essential that a proper knowledge of the kinds of mechanisms involved be understood. If a prediction is to be made, based upon a sampling of the individual components or of the interactive components, it is necessary for the kinds of mechanisms developed and sensed by the sampling procedures to be similar in essence to those identified as responsible for the actual system behaviour needed to be predicted.

If the sampling or predictive techniques do not mirror or generate mechanisms similar to that provoked by the actual or real system to be predicted, it becomes immediately obvious that the ability to predict the actual or real system becomes severely hampered. The further one departs from the *similar mechanism* requirement, the less is one's ability to successfully predict the behaviour of the real system.

If one were to depart from the ideal prediction problem requiring modelling of the actual field situation to small test tools, the kinds of field testing tools such as those shown in Fig. 3 need to be properly assessed with regard to their appreciation of the actual mechanics of the real system itself.

To reduce the problem to its most simple form, and to allow for the greatest ease in development of similarity modelling, the concept of energy conservation and its application provides for the most attractive form of comparison performance. The energy expenditure details given in Figs. 1 and 2 portray the kinds of energy fields or quantities demanded by the wheel and track-terrain interaction problem, together with the

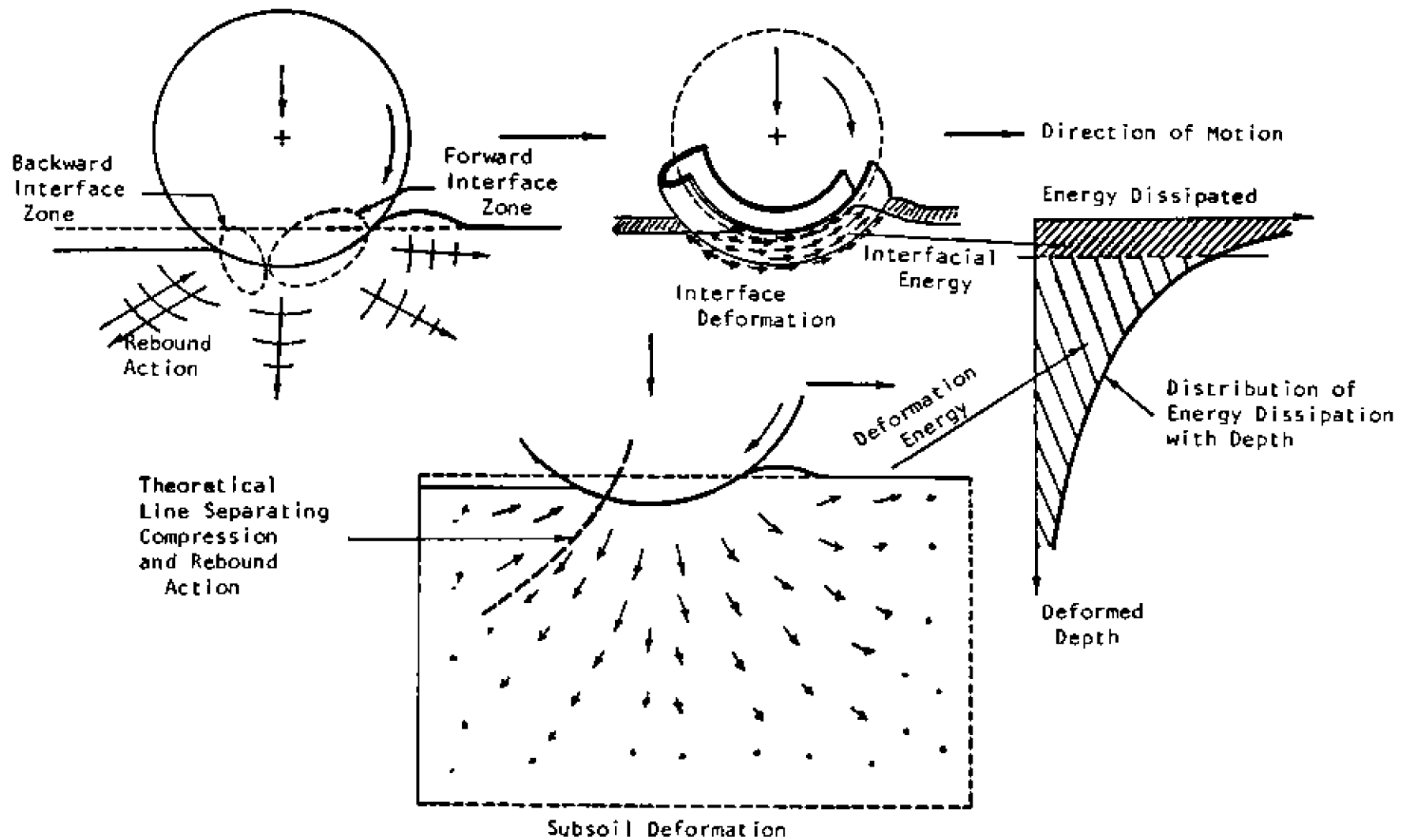


Fig. 1 Response Substrate Behaviour and Energy Transfer beneath a Moving Rigid Wheel.

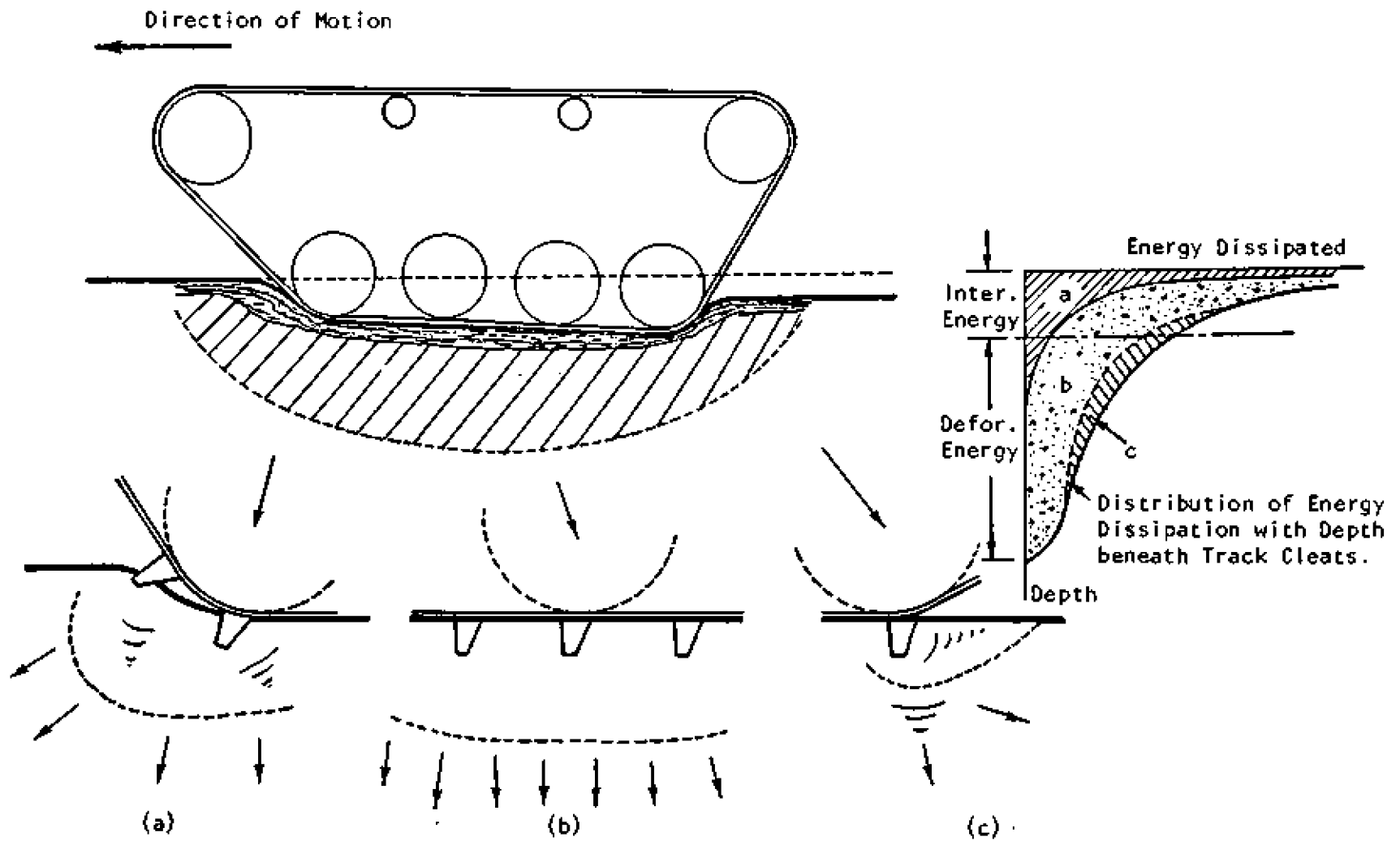


Fig. 2 Response Substrate Behaviour and Energy Transfer beneath a Moving Track.

essential items produced by the sensing devices. Note that because of the fact that energy is a scalar quantity, there is no particular requirement for a duplication of the strain or strain rate fields, the stress or the deformation fields associated between the real system and the test devices.

As can be noted from Fig. 3, all the tools produce deformation fields, for which the energy associated with the deformation of the soil can be obtained. How these relate as direct quantities to the wheel-terrain or track-terrain problem is one which requires analysis of the test results using a modelling procedure which reflects the actual mechanics of the running gear-terrain interaction, i.e. there must be a supportive analytical theory which utilizes energetics in the formulation of the mobility equation.

Note that the energy terms per se do not provide one with an actual direct prediction of mobility. The terms provide an appreciation of the amount of energy expended in shear distortion and in deformation of the soil. With reference to the sensing tools, substrate deformation energy evaluation is obtained either through the penetration of the cone or vane-cone devices, or direct bearing of loading plates. One might equate the subsoil deformation aspects of the phenomenon material for a static loading situation.

Recognizing that the running gear-soil interaction problem requires both deformation and slip for a complete appreciation of the mechanics of the vehicle-terrain interaction problem, we observe that the slip requirement is not generally directly met by any of the tools.

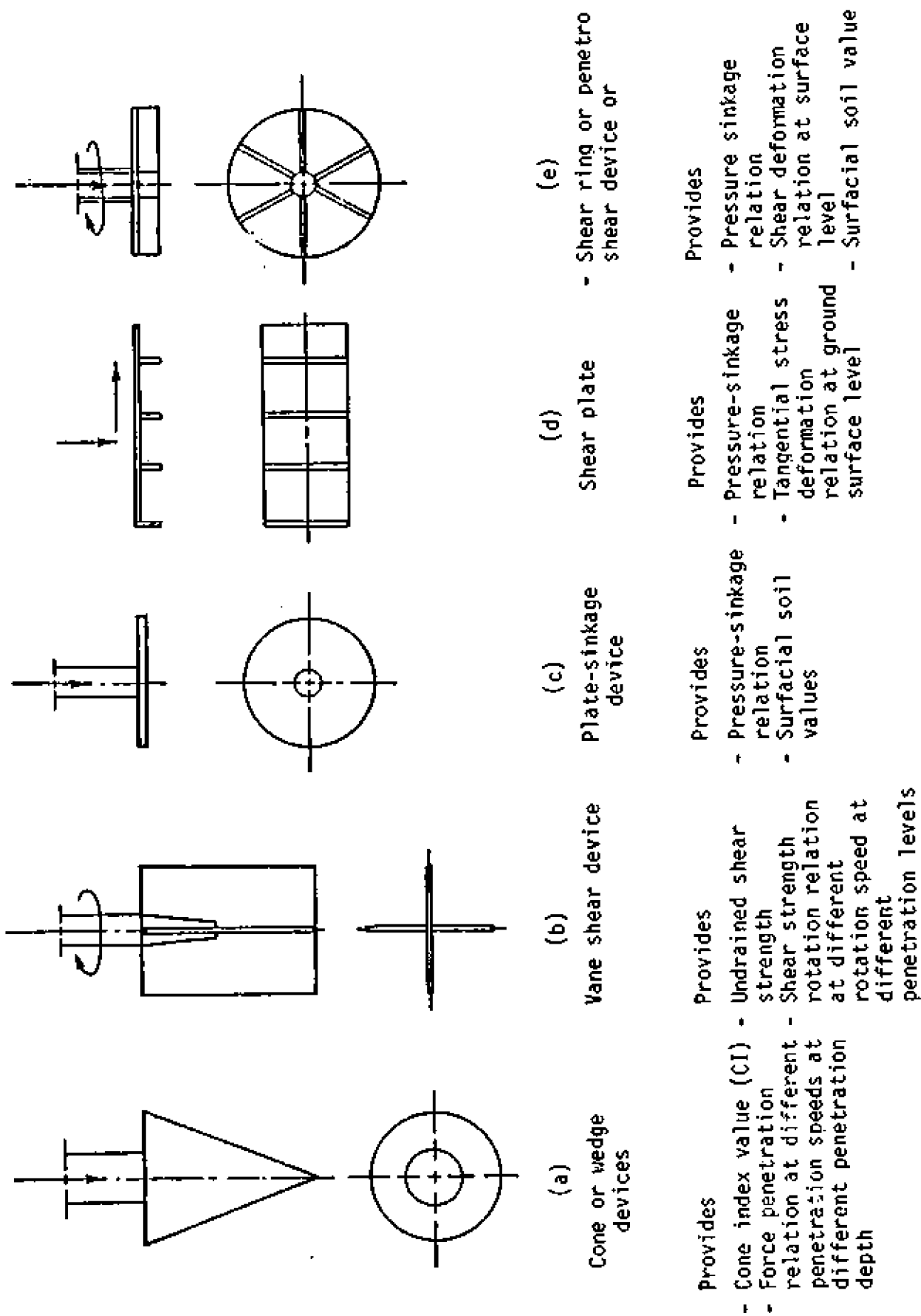


Fig. 3 Conventional Devices used or recommended in the Field of Trafficability

However, the generative mechanisms needed to provide for computational success in determination of slip energy can be obtained from a knowledge of the shear strength of the material. The use of measured shear stresses for computation of slip energy loss requires the establishment of a proper analytical framework.

Suffice it to say that the applicability of any sensing tool insofar as mobility prediction is concerned, depends not only on the measurements made by the tool, but also on the manner of utilization of the measurements consistent with the analytical framework describing the vehicle-soil interaction problem. This aspect of the problem cannot be overstated.

THE VANE-CONE DEVICE

The vane-cone device shown in Figs. 4 or 5 was developed with the knowledge that the two prime parasitic energy components are compression and interfacial energy loss, as indicated in Figs. 1 and 2. In addition, the requirement for simplicity in utilization and equipment portability dictated that the instrument be sufficiently simple.

Figure 6 shows the kinds of mechanisms developed with application of the vane-cone device. As in the cone aspect of the device, the kinds of mechanisms developed due to penetration of the cone are not unlike those previously presented by Yong et al. (1972). Thus only the deformation energy component is sensed. As shown previously by Yong et al. (1972), the cone, in essence, does not develop a significant shear stress at the interface if the surface of the cone is smooth and if the

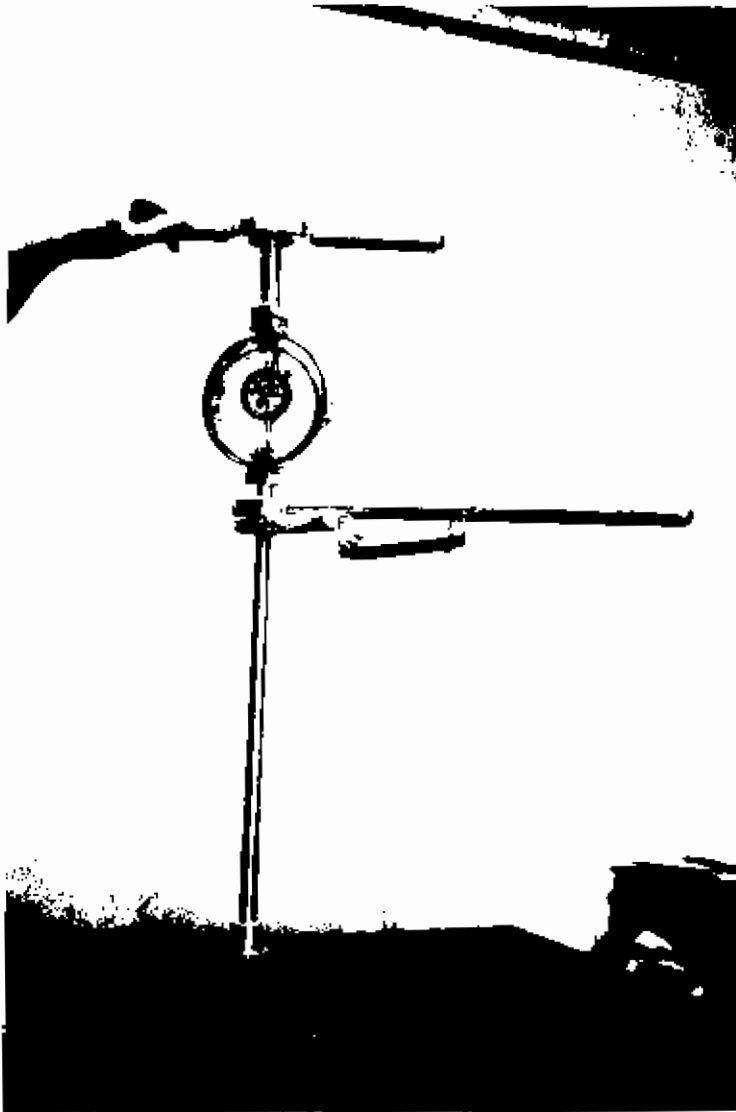


Fig. 4 Photograph of Vane-Cone Device for Field Test

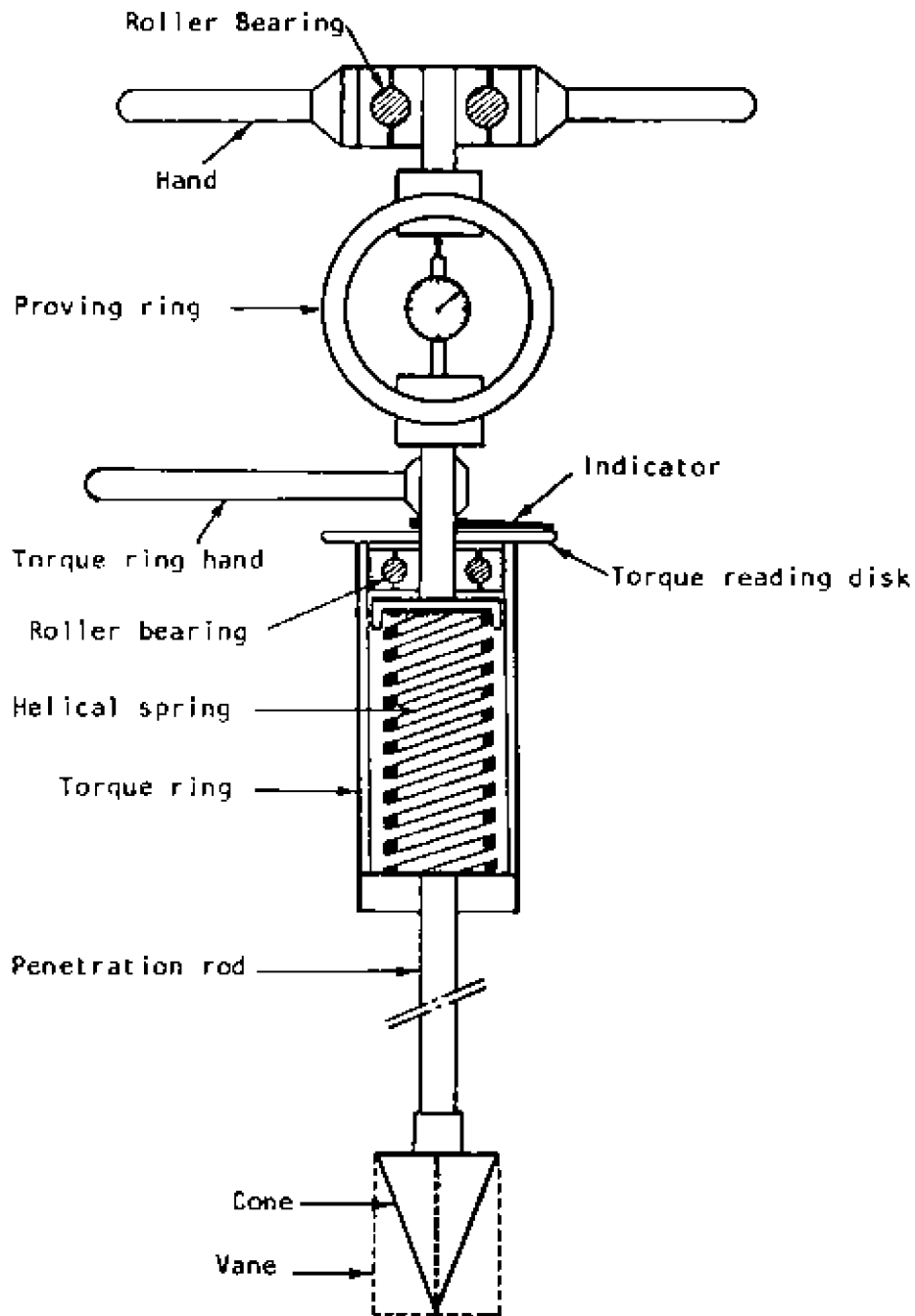


Fig. 5 Vane-Cone Device for Field Test

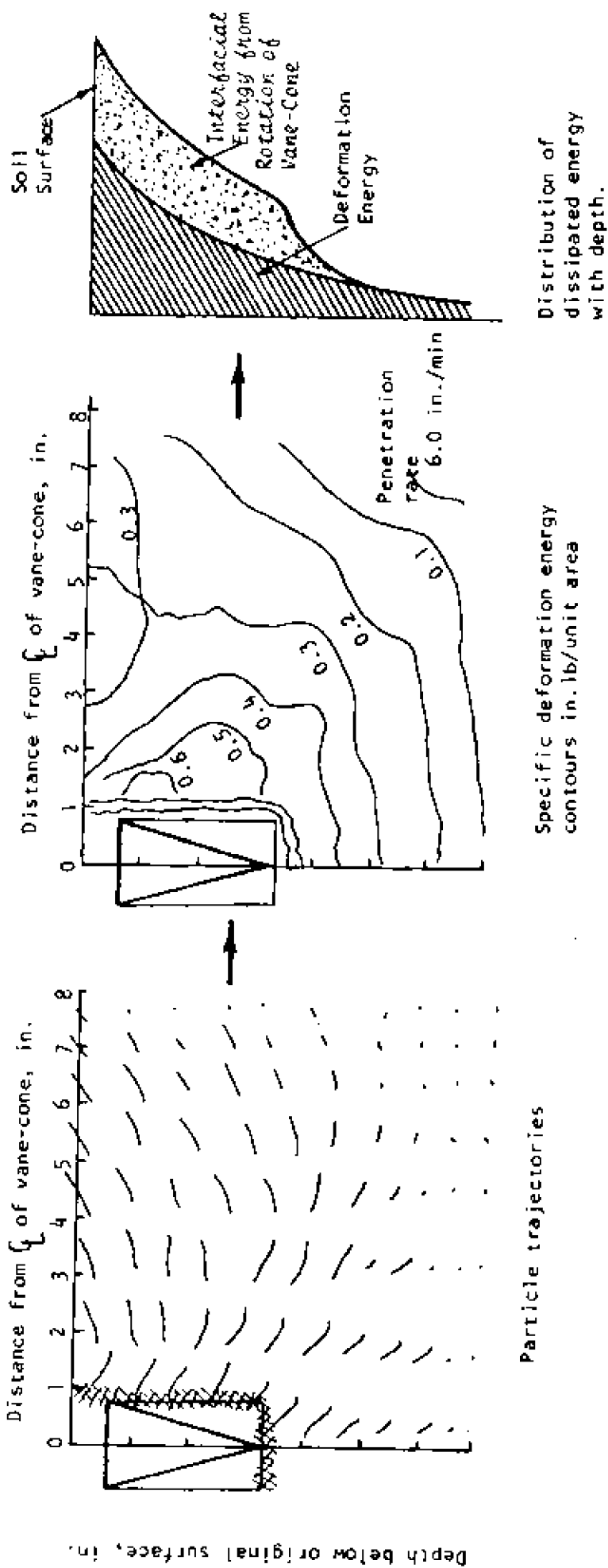


FIG. 6 Soil particle trajectories and corresponding dissipative energy field developed by penetration of a 30° vane-cone penetrometer.

soil is frictionless. Thus one is left with devising a technique which would provide for slip energy loss characterization. Initial test results using the vane-cone device for assessment of cone penetration and shear as separate or combined tests have been previously reported by Yong et al. (1975). These preliminary tests have lent support to this present study for application to mobility prediction using a set of standard analytical procedures.

The vane portion of the vane-cone device will provide a shear strength evaluation of the soil if the vane-cone is rotated. The technique requires that the cone be penetrated to the required depth and maintained at that depth for rotation of the vane. Note that the vane portion of the vane-cone device is in actual fact not dissimilar to the commercially available vane shear devices used in the geotechnical engineering practice. It is common practice in geotechnical engineering to use vane shear values for evaluation of soil properties and strength. The resistance values or shear strength measurements obtained thereby can be converted into slip energy loss relationships.

The procedure for application of the vane-cone device requires that the cone be penetrated into the soil at a rate less than 72 in./min. Note that the penetrating force for the vane-cone is almost identical to that of the cone [by itself], and to all intents and purposes, one would consider the penetration of the vane-cone equal to the cone. At the required specified depth of penetration, the cone is maintained at that depth of penetration whilst being rotated to produce the vane shear sensing aspect of the vane-cone device. Note the importance for the requirement for the vane-cone to be maintained at that position with no further

penetration whilst the vane-cone is being rotated, since the analyses performed must relate soil strength to the depth of soil stratum sampled. The rate of rotation of the vane-cone is conditioned by the shear resistance of the soil. If desired, the vane-cone may be further penetrated into the soil and the procedure for vane shear repeated at a lower depth whilst maintaining the cone at the new penetrated depth.

The vane-cone mechanics can be developed by dividing the device into two components as shown in Fig. 7. By defining the forces acting on each of these components and using the principle of superposition, the total combined loads, and hence the total energy transfer, can be predicted.

In the present case, and for the purpose of simplifying the analyses, it is assumed that the penetrometer remains in approximately the same vertical position during rotation. This may not be strictly true and may not be fully controlled in the field because of the inevitable soil relaxation effect. It has been shown from laboratory experiments that the relaxation effect is very small for the situation where the penetrometer is fully embedded in the soil.

The measured values of both cone and cone component of the vane-cone [Fig. 7] with the same dimension have been previously shown to be equal by Yong and Youssef, (1977). The soil behaviour around the vane component is considered to be the same as that around the vane-shear device, with the proper accounting for the effect of the vertical load imposed by the cone component during rotation.

Based on the above discussion and on the static systems

- F = Total penetration resistance
- M = Total torsional resistance
- P' = Penetration resistance due to cone component
- P'' = Penetration resistance due to vane blades
- p = Radial stress due to cone component
- τ = Shear resistance due to cone penetration force
- τ' , τ'' = Shear stresses due to torsional resistance
- C_a = Adhesion between soil and blade

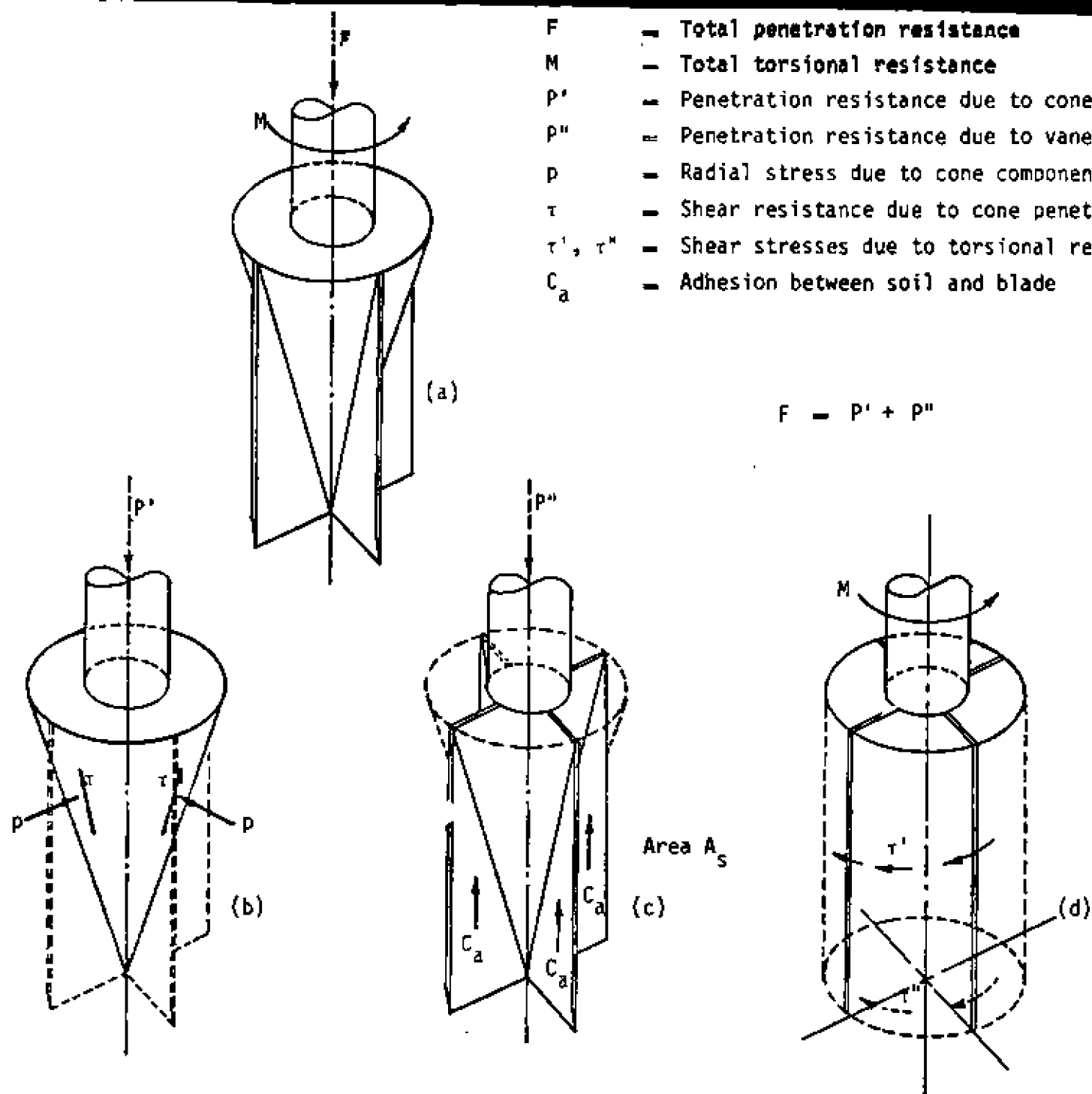


Fig. 7 Vane-Cone Device Components

illustrated in Fig. 7, the penetration and rotation resistances can be written in the following form:

$$F_y = \lambda \left[\left[\begin{array}{l} \text{vertical components of radial and tangential} \\ \text{stress (P \& \tau_s) integrated over cone or cone} \\ \text{component surfaces [Fig. 7-b].} \end{array} \right] + \right. \\ \left. n C_a A_s \text{ [Fig. 7-c]} \right] \\ F_x = f(F_y \text{ and penetrometer geometry}) \quad (1)$$

$$T = (2\pi \int_{y=0}^H f(y) \cdot \tau_{t_1} \cdot d^2 \cdot dy) + (2\pi \int_{r=0}^d f(x) \cdot \tau_{t_2} \cdot r^2 \cdot dr)$$

where

F_y , F_x , T = vertical, horizontal and torsion resistances, respectively,

P = radial pressure around cone or cone component surface,

τ_s = tangential stress around cone or cone component surface,

τ_{t_1} = maximum tangential resistance at the outer vane-surface, Fig. 8,

τ_{t_2} = maximum tangential resistance at the horizontal surface beneath the vanes, Fig. 8,

$f(\)$ = function of ,

C_a = adhesion between soil and vane blades, Fig. 7, assuming the soil is pure cohesive material,

H = cone or vane height,

d = cone or vane radius,

y = cone or vane height measured from the tip,

r = cone radius at the height y ,

A_s = surface area of one side of vane blade, and

n = number of blade surface.

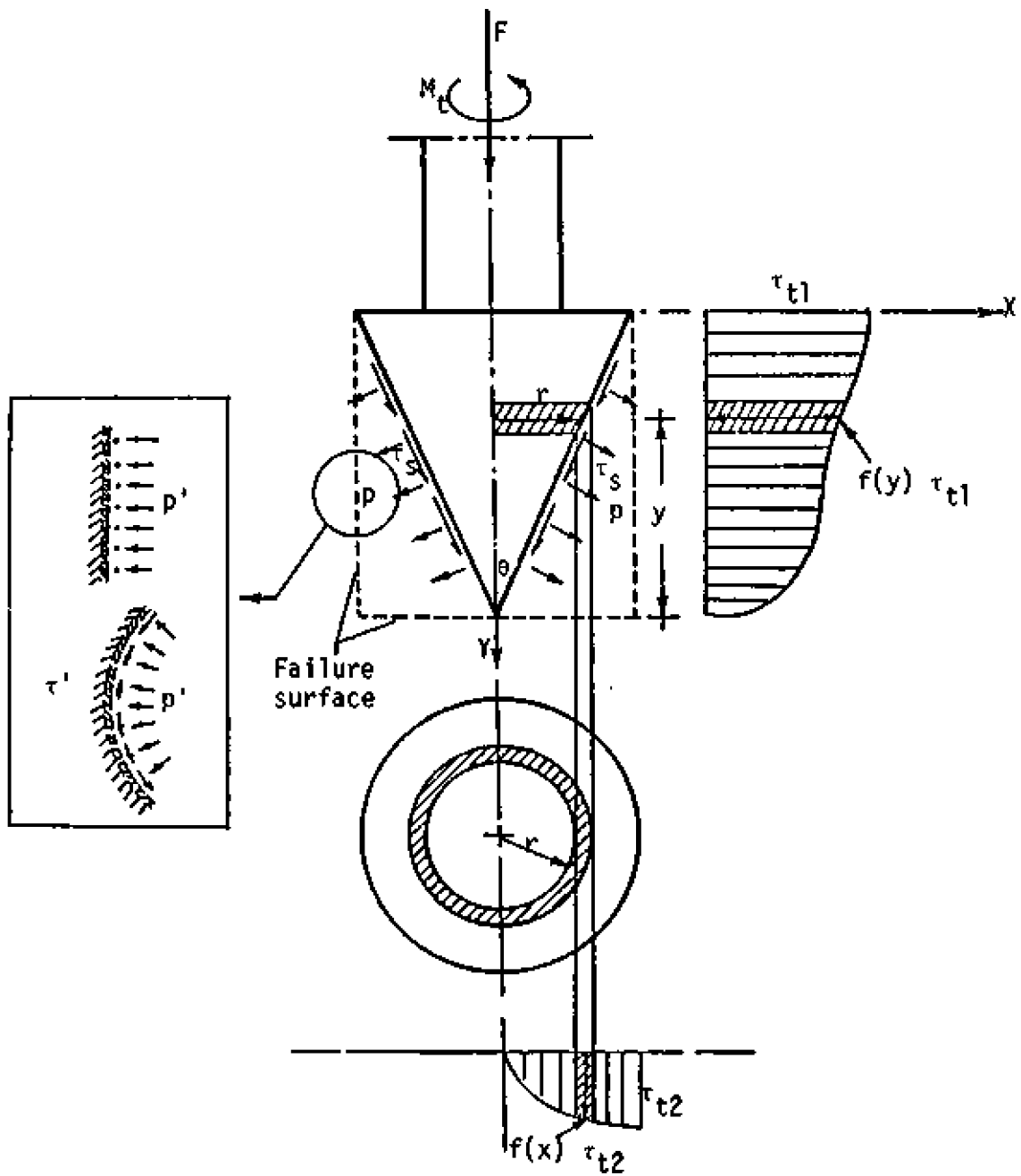


Fig. 8 Shear Stress Distribution around and beneath Vane-Cone Device

For the purpose of predicting the radial and tangential stress distribution required for the above analyses around the cone and around the vane-cone device respectively, a proper theoretical analysis is used. This theoretical analysis is developed based on the plasticity analysis and is similar to that used by Yong and Chen, (1976). The detailed analysis is given by Youssef, (1977).

For a cohesive material which obeys Tresca yield criterion, the equilibrium plastic equation can be written in cylindrical coordinates as:

$$\cos 2\psi \frac{\partial \psi}{\partial y} + \frac{\partial \chi}{\partial x} - \sin 2\psi \frac{\partial \psi}{\partial x} = \frac{-\sin \psi \cos \psi}{y}$$

$$\frac{\partial \chi}{\partial y} + \sin 2\psi \frac{\partial \chi}{\partial y} + \cos 2\psi \frac{\partial \psi}{\partial x} = \frac{\cos^2 \psi}{y}$$
(2)

where

x and y = axial and radial coordinates,

ψ = angle between the major principal stress and x -axis,

$$\chi = \frac{\frac{1}{2}(\sigma_1 + \sigma_2) - \gamma x}{2c}$$

σ_1, σ_2 = major and minor principal stresses,

c = cohesion, and

γ = soil density.

A numerical solution of Eq. (2) is sought in terms of the method of characteristics. Once the values of the variables ψ and χ are obtained along the penetrometer contact surface, and with the help of Eqs. (1), it becomes possible to predict:

- (1) the radial and tangential stress distribution around the penetrometer,
- (2) the force penetration relation, and
- (3) the dissipated energy beneath and around the penetrometer at different penetration depths.

From Eq. (1) and the stress distribution obtained from Eq.(2) [Youssef, (1977)], the torque resistance relation can be written as:

$$T = F \tan \phi \left(\frac{d}{2} \cot \frac{\theta}{2} + \frac{d}{2} \right) + C \left(\frac{\pi}{2} d^3 + 2\pi d^2 H \right) \quad (3)$$

where

F = vertical force,

θ = penetrometer apex angle.

In the above analysis, the effect of the volume change is assumed to be small. This is true when the penetrometer remained approximately in its vertical position during rotation.

Equation (3) is a relation between rotation resistance T , and shear strength parameters C and ϕ in the existence of a vertical force, F . This equation gives a straight line relation between rotation resistance T and penetration resistance F . This straight line will intersect the force axis F at a distance equal to $C \left(\frac{\pi}{2} d^3 + 2\pi d^2 H \right)$ from the origin, and its slope with respect to the torque axis is $\tan \phi \left(\frac{d}{2} \cot \frac{\theta}{2} + \frac{d}{2} \right)$. Thus, by imposing another vertical load and measuring the corresponding torsion resistance, the shear strength parameters can be obtained.

In Fig. 9, the vertical resistance and the corresponding torque resistance at different penetration levels is shown; they vary with the

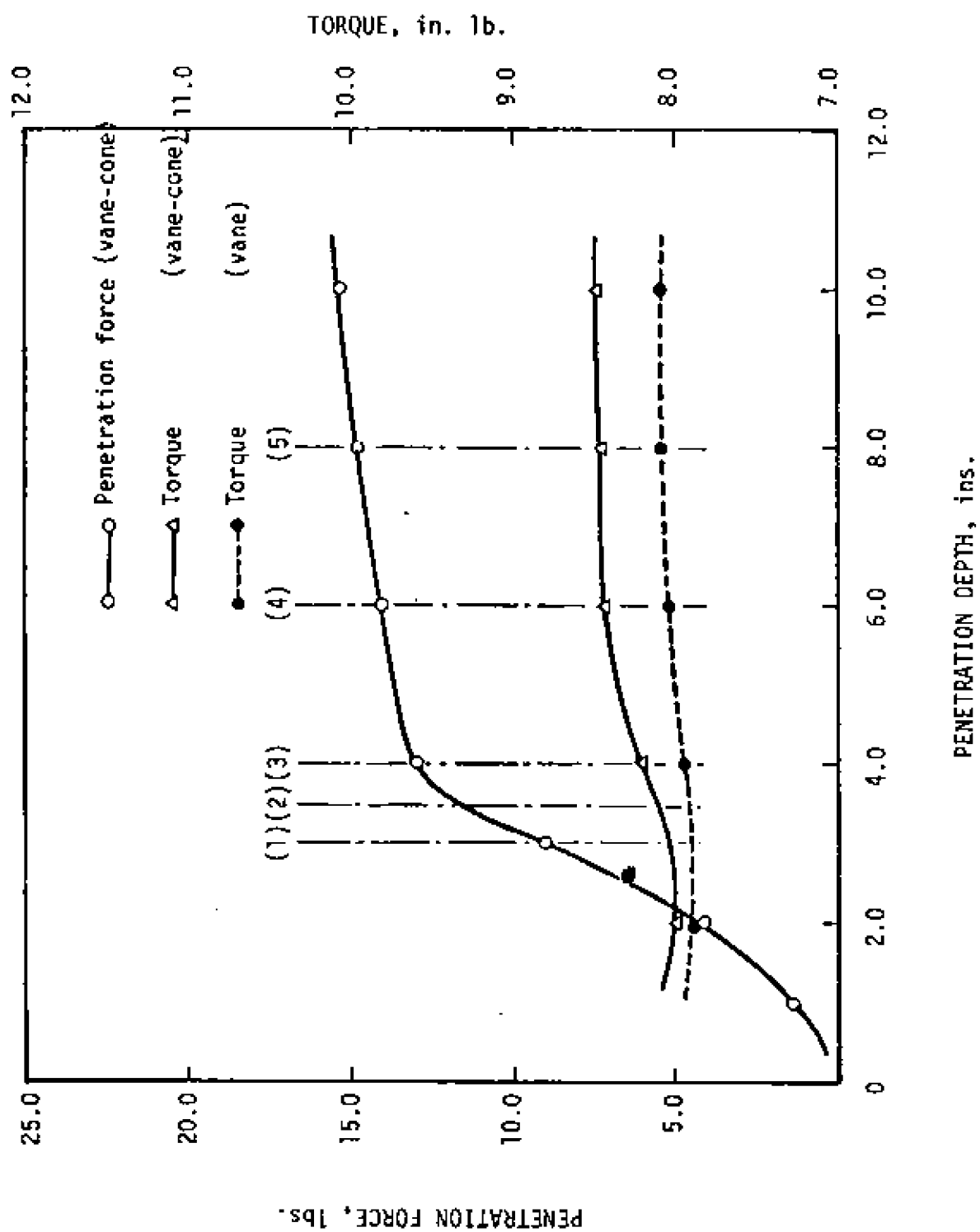


Fig. 9 Penetration Force and Torque Resistance vs Depth of Penetration

variation of soil or other substrate material resistance at different depths of penetration. Based on these results, Eq. (3) was plotted in Fig. 10. In the case of soil material, the shear strength parameters C and ϕ can thus be obtained. These values appear to correspond well with triaxial test results.

VANE-CONE PREDICTION METHOD

It is recognized that the actual wheel or track performance, in regard to subsoil deformation, is influenced by many factors such as wheel or track dimensions, loads, contact surface characteristics and angular and translational velocities. This performance may be discussed in terms of energy transfer mechanisms at the wheel or track interface as discussed in the initial portions of this paper.

The energy transfer component associated with the subsoil deformation must obviously depend on the mechanics of transfer at, and beneath, the interface and is thus related directly to the interface input energy component. The procedure requires an analysis of the overall problem in terms of the rationale for partitioning the components of parasitic energy.

It is desirable to separate the vane-cone method of prediction into two approaches:

- (a) Rigorous approach which considers most of the variables and affecting the real problem.

This might require a more detailed examination of experimental measurements coupled with theoretical analyses. This

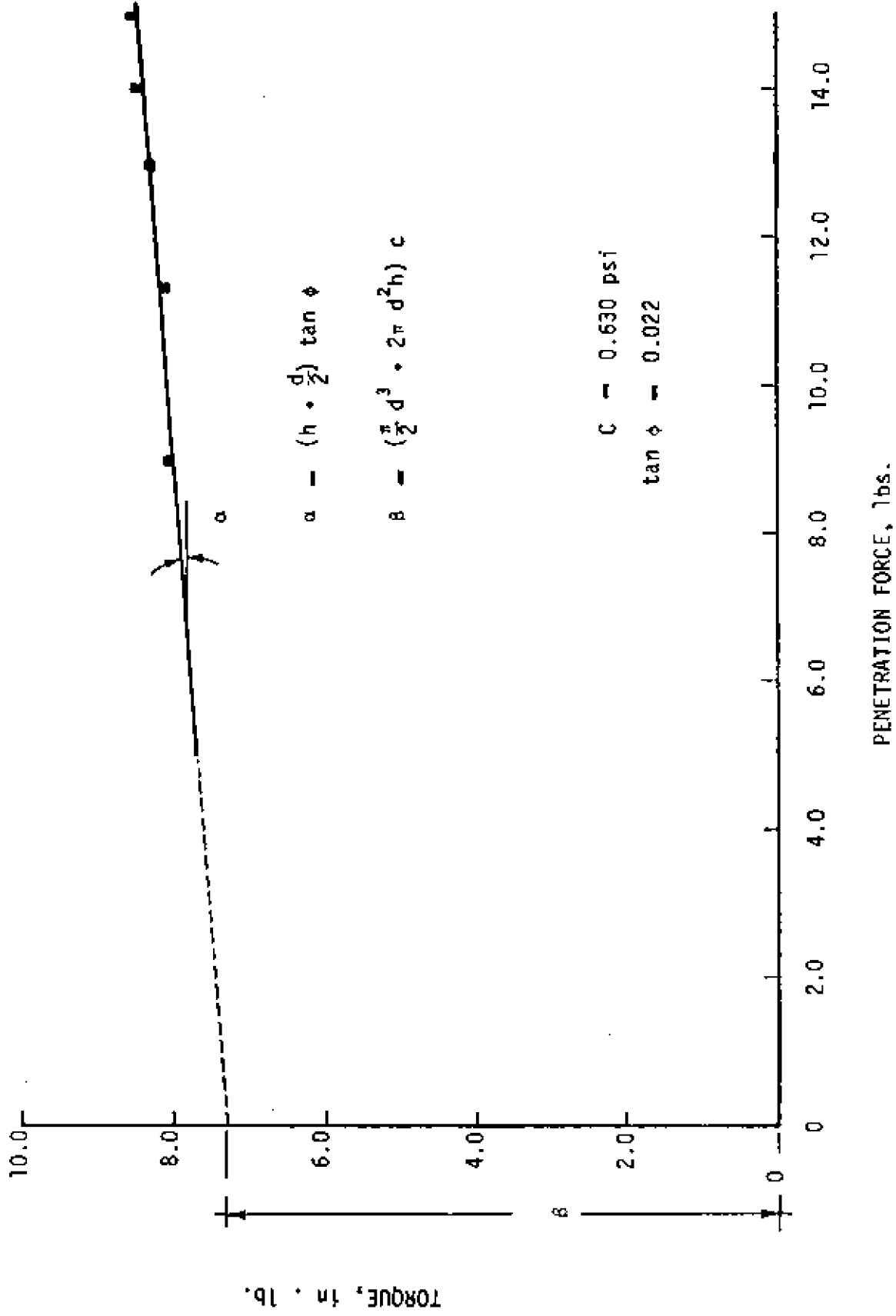


Fig. 10 Graphical Solution for Equation (3)

approach is not developed in this paper. The detailed procedures, requirements etc. of this rigorous approach are discussed separately in another report.

- (b) "Simple" approach using approximate simplifying equations developed as a result of both theoretical and experimental analyses. The first order simplification of the working equation is shown here for wheels moving over soft soil. Note that these can be used directly with the simple vane-cone device. Note also that continued development and generalization of such type of equations for all vehicles and all types of soils is continuing.

The simple approach for vane-cone prediction for wheel performance moving over soft soilⁱⁱ can be achieved using the following equations:

Input Energy Prediction, I.E.

$$I.E. = \frac{mbd}{2} \left[\frac{W^2(1+2S)^2}{N_c p^2 b^2} + \delta d \right]^{\frac{1}{2}} \cdot \tau \cdot \omega \quad (4)$$

Slippage (or Interfacial) Energy Prediction, S.E.

$$S.E. = \frac{mbd}{2} \left[\frac{W^2(1+2S)^2}{N_c p^2 b^2} + \delta d \right]^{\frac{1}{2}} \cdot \tau \left(\omega - \frac{2V_c}{0.935d} \right) \quad (5)$$

Deformation Energy Prediction, D.E.

$$D.E. = b \cdot V_c \cdot [A]_0^Y \quad (\text{See Fig. 11}) \quad (6)$$

ⁱⁱ Note that corresponding relationships for mobility performance on snow insofar as vane-cone application is still under development.

where

$$\gamma = K \left[\frac{W^2}{N_c p^2 b^2 d} \right] + \alpha e^{\beta \left(\frac{h}{2r} \right)}$$

Pull Energy Prediction, P.E.

$$P.E. = I.E. - S.E. - D.E. \quad (7)$$

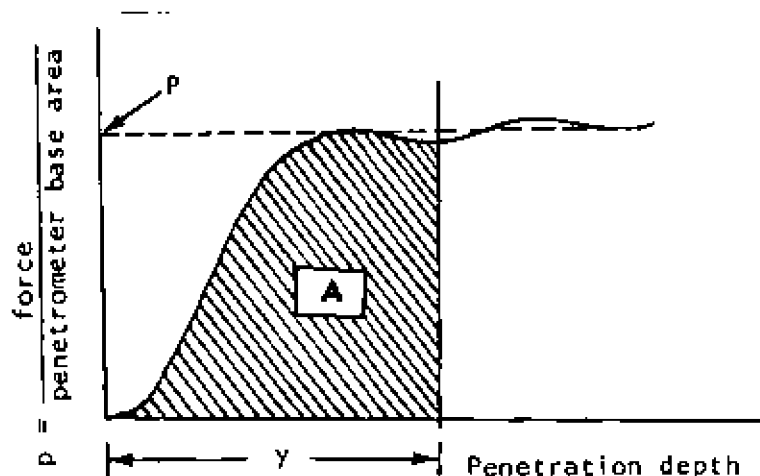


Fig. 11 Pressure-Penetration Diagram for Vane-Cone Penetrometer.

where^{*}

- W = wheel load,
- p = pressure beneath the penetrometer,
- b, d = wheel width and diameter,
- h, r = penetrometer height and radius,
- δ = tread height,
- S = slip,
- V_c = translational velocity,
- ω = angular velocity,
- τ = tangential shear stress obtained at the outer edge of the vane component,
- m = factor takes the effect of backward contact area equal to 1.31,
- N_c = bearing stability factor which is dimensionless and equal to 0.225 for φ = 0,

^{*} Note that the items listed are readily obtained in measurements.

K, α, β = dimensional factors obtained from viscoplasticity analyses (semi-analytical analyses) for the purpose of deformation energy prediction. For cohesive material, $\phi = 0$ and in the case of lb in. units, $K = 1.21$, $\alpha = 0.97$ and $\beta = 0.230$.

COMPARISON OF DRAWBAR PULL PREDICTION RESULTS USING THE THREE SENSING DEVICES

Three types of wheels were used in the tow bin tests on a soft clay soil.^{**} These were:

- (a) a polished aluminum wheel,
- (b) a rigid wheel with its contact surface coated with a 1/8 inch thick rubber, and
- (c) the same rubber wheel coated with a tread surface. (tread height = 1/2 inch).

Three loads were used for all the tests with these three types of wheels in the tow bin, using techniques and measurement procedures previously reported by Yong and Windisch (1970). The loads were 34 lb, representing the weight of the wheel itself, 54 lb, and 74 lb. The size of the wheel was 13.5 inches in diameter, and 3.75 inches wide.

Figures 12, 13 and 14 show comparisons between the laboratory measured and predicted values using the vane-cone device, the vane-cone penetrometer [with the power number approach for analysis, Melzer (1972), Yong and Youssef (1977)], and the technique using plate and shear ring device.

^{**} Note that because of size limitations, no snow mobility tests could be conducted in the laboratory. Field snow tests are presently [February 1978] being conducted and will be reported on at a later time.

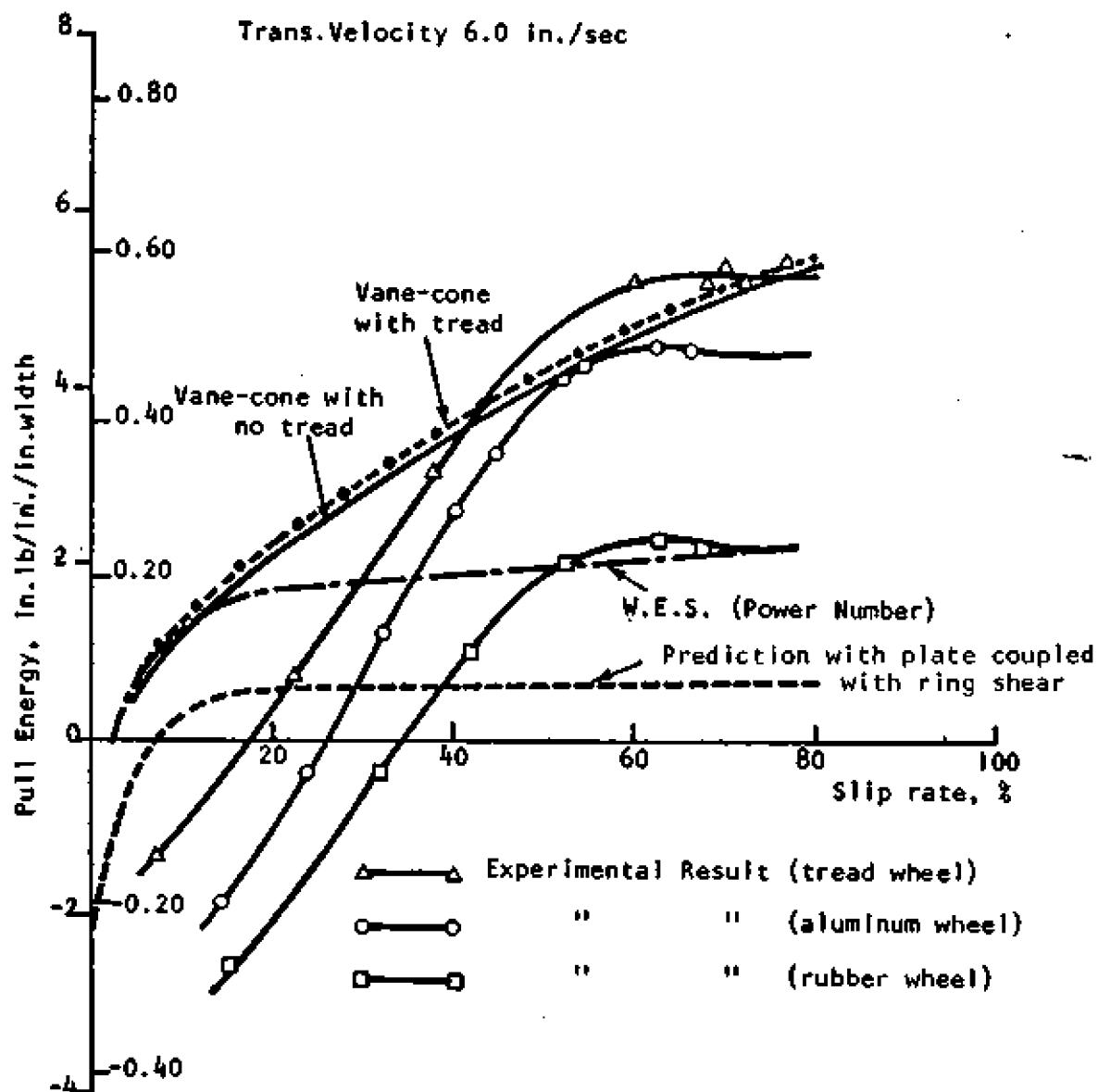


FIG. 12 Measured and predicted pull energy using Bevameter, W.E.S. Power Number, and approximate Vane-Cone equations. (for 34 lb wheel load)

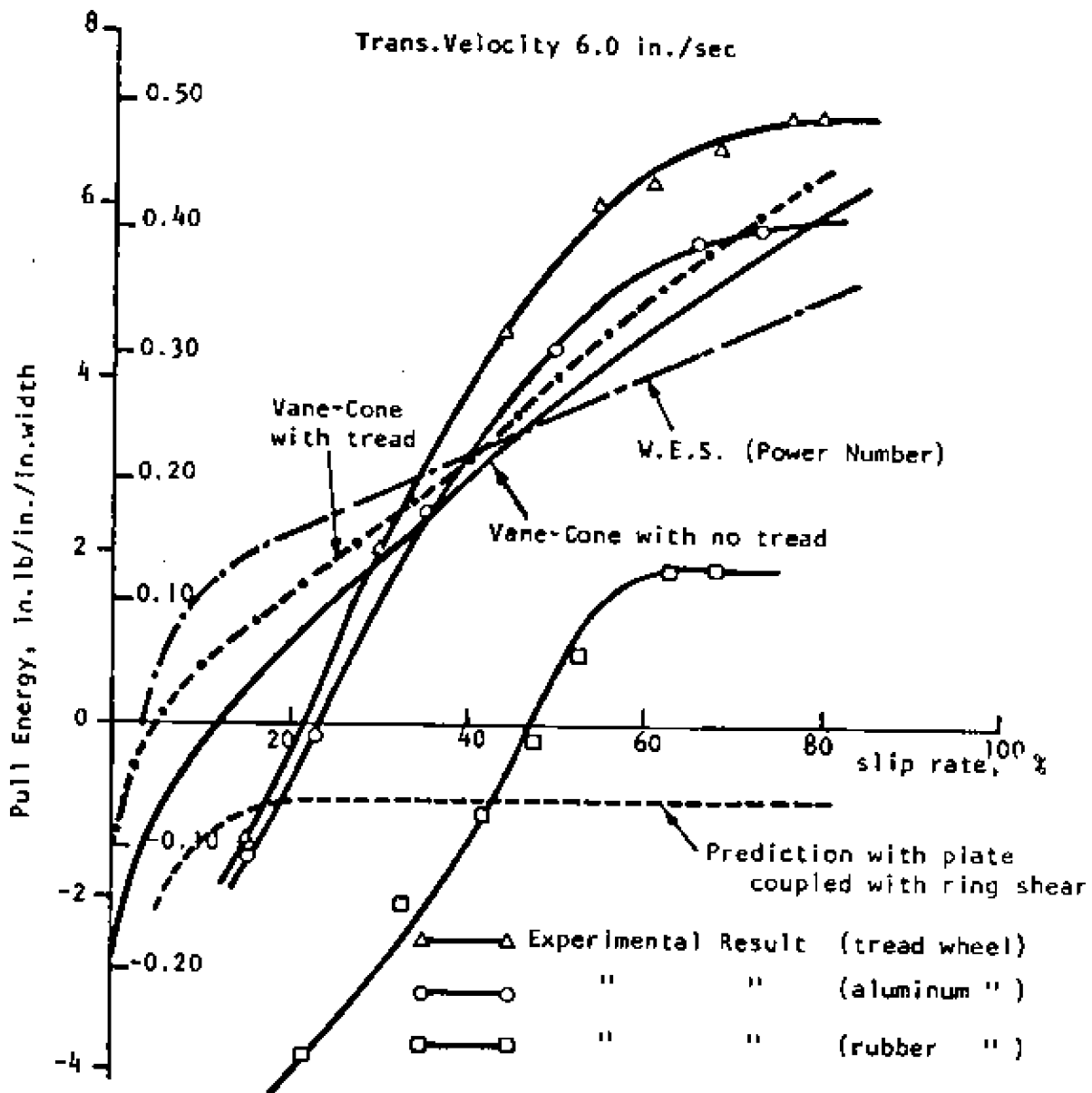


FIG. 13 Measured and predicted pull energy using Bevameter, W.E.S. Power Number, and approximate Vane-Cone equations.
(for 54 lb wheel load)

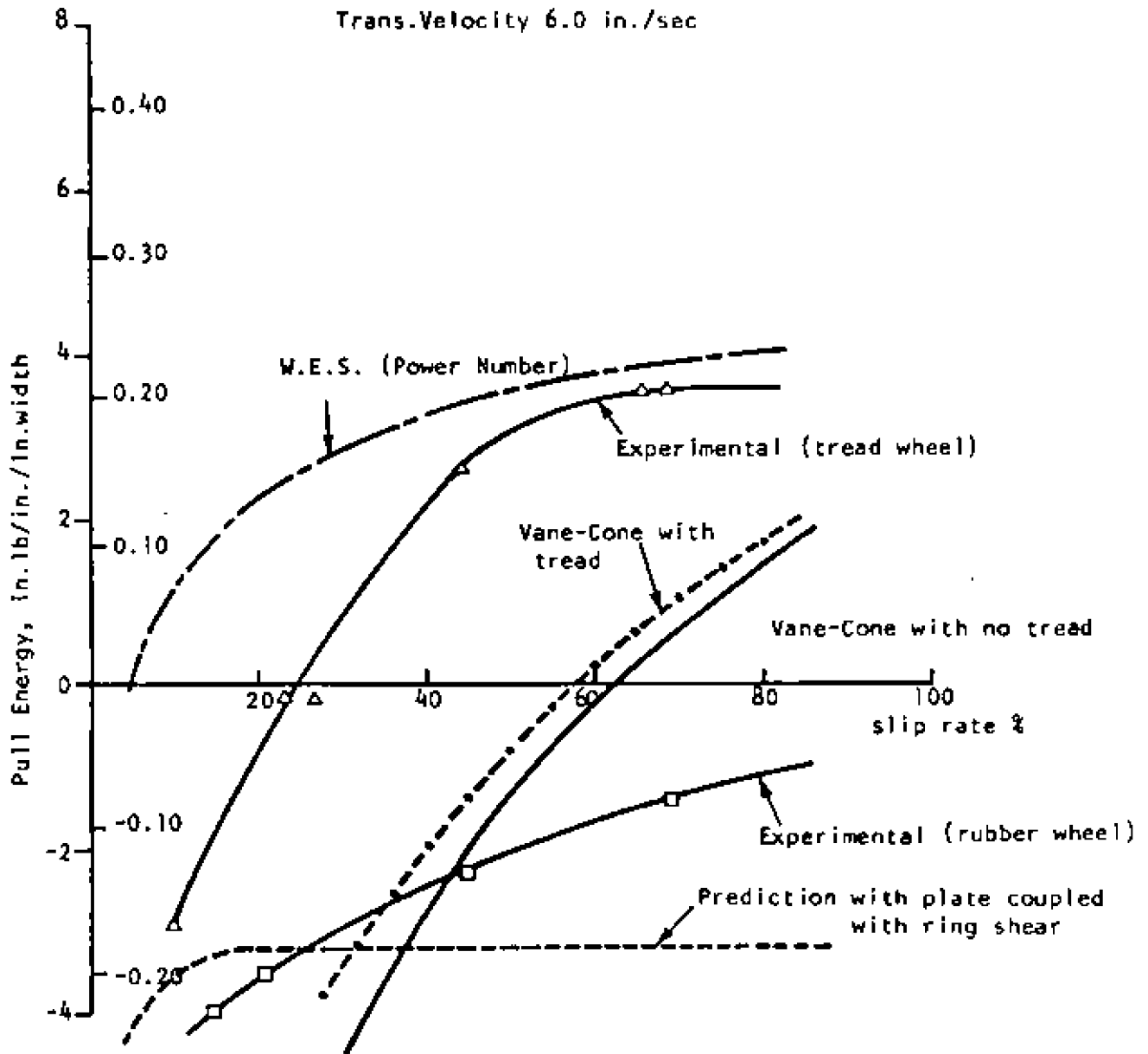


FIG. 14 Measured and predicted pull energy using Bevameter, W.E.S. Power Number, and approximate Vane-Cone equations.
(for 76 lb wheel load)

CONCLUDING REMARKS

As can be seen from the Figures show, the ability to predict the measured drawbar pull in the tow bin tests using soft soil as the terrain material, with the kinds of measurements made with the vane-cone device are indeed more favourable in comparison to some others. The associated analytical framework for utilisation of the vane-cone results - i.e. utilisation of the data in terms of energetics provides for a method of analysis and prediction which responds more closely to the actual problem at hand - especially if the higher level of sophistication of analysis is used. Thus it is not surprising that the data obtained with the vane-cone device, together with the utilisation of energetics as a method of analysis can indeed provide for a closer predictive correlation with the results obtained in actual tow bin tests using soft soil.

The results of the study indicate that it is most important to obtain proper simulation from these test devices of the mechanics of vehicle-terrain interaction if a feasible prediction for mobility is to be made. We note that whilst measurements can be obtained from these instruments which may or may not be pertinent to the actual mechanics of vehicle-terrain interaction, the other important consideration for mobility prediction is the actual analytical framework within which these measurements must participate. Thus, it is not only the instruments that are used that are important for prediction of mobility, but also the method of application of the measurements obtained from these tools for analysis and prediction of mobility. Where the

proper appreciation of the actual system problem is obtained, both from a measurement and an analytical point of view, a viable prediction for mobility can be reasonably obtained.

ACKNOWLEDGEMENTS

This study was conducted under contract arrangement with the Department of Supply and Services - with project administration from the Mobility Section of Defence Research Establishment Ottawa (DREO). The assistance and input given by the Project Officer, Mr. I. S. Lindsay, Earth Sciences Division, are acknowledged.

REFERENCES

1. K. J. Melzer, *Power Requirements for Wheels operating in Fine-grained Soils*, Paper No. 72-617. Winter Meeting, American Society of Agricultural Engineers, Chicago, Illinois. (1972).
2. R. N. Yong and C. K. Chen, *Cone Penetration of Granular and Cohesive Soils*, J. Engineering Mechanics Division, EM2, pp. 345-363. (1976)
3. R. N. Yong, C. K. Chen and R. Sylvestre-Williams, *A Study of the Mechanics of Cone Indentation and its Relation to Soil-Wheel Interaction*, J. Terramechanics, Vol.9, No.1, pp.19-36. (1972).
4. R. N. Yong and E. J. Windisch, *Determination of Wheel Contact Studies from Measured Instantaneous Soil Deformations*, J. Terramechanics, Vol.7, Nos.3 and 4, p.57. (1970).
5. R. N. Yong and A. F. Youssef, *Prediction of Mobility and Drawbar-Pull in Tow-Bin Tests using Cone, Vane-Cone and Bevameter-type Tools*, Soil Mechanics Series No. 37, McGill University, Montreal, Canada. (1977).
6. R. N. Yong, A. F. Youssef and E. A. Fattah, *Vane-Cone Measurements for Assessment of Tractive Performance in Wheel-Soil Interaction*, Proc., Fifth Int. Conf. ISTVS. Detroit, Vol.3, p.769. (1975).
7. A. F. Youssef, *Energy Analysis for Vane-Cone Prediction of Wheel-Soil Interaction*, Ph.D. Thesis, McGill University, Montreal. (1977).

PREDICTION OF TYRE PERFORMANCE ON SOFT SOILS
RELATIVE TO CARCASS STIFFNESS AND CONTACT AREAS

by

R. N. Yong, P. Boonsinsuk and E. A. Fattah

prepared for

SIXTH INTERNATIONAL CONFERENCE
I.S.T.V.S.

Session 1. - Recent Theoretical Developments

Vienna

August 1978

PREDICTION OF TYRE PERFORMANCE ON SOFT SOILS RELATIVE
TO CARCASS STIFFNESS AND CONTACT AREAS

by

R. N. Yong,¹ P. Boonsinsuk² and E. A. Fattah³

ABSTRACT

The development of analytical techniques for evaluation and analysis of performance of tyres on soft ground, requires the properties of the tyres for accurate prediction of tyre-ground interaction. This study addresses the problem of prediction of tyre-soil performance by considering the interaction between tyre and soil in terms of energetics - i.e. the mechanics of energy transfer.

If a proper analysis of participating components in a tyre-soil interacting problem is to be made - on the basis of the mechanics of energy transfer, i.e. conservation of energy - it then becomes necessary to provide a means for evaluation of load-deformation and elastic properties of the tyres. In this study, three model tyres have been tested to determine properties relating to carcass stiffness and contact area development on rigid pavement, and stiff and soft soils. The contact areas developed for the tyres examined are evaluated with respect to the carcass stiffnesses of the tyres.

¹ William Scott Professor of Civil Engineering and Applied Mechanics, and Director, Geotechnical Research Centre, McGill University, Montreal, Canada.

² Graduate Research Assistant, Department of Civil Engineering and Applied Mechanics, McGill University, Montreal, Canada.

³ Research Associate, Geotechnical Research Centre, McGill University, Montreal, Canada.

The contact areas of the tyres tested, on rigid pavement, and on stiff and soft soils, are examined in relation to tyre load-deformation characteristics. The contact pressures obtained in tyre reactions with the various bearing surfaces are described accordingly and used as input to the evaluation of tyre-soil interaction.

INTRODUCTION

In the development of analytical techniques for evaluation and analysis of performance of tyres on soft ground, one of the necessary requirements for accurate prediction of tyre-ground interaction is the properties of the tyres. Following on the recent developments involving analyses of wheel-soil interaction using energetics [Yong and Webb, (1969)], and the finite element method (FEM) of analysis for application to the prediction of wheel performance, [Yong and Fattah, (1976)], it is seen that the prime tyre properties need proper characterization and specification for knowledge of energy expenditure, and as input to the FEM analysis.

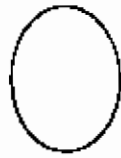
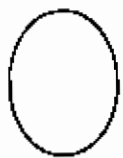
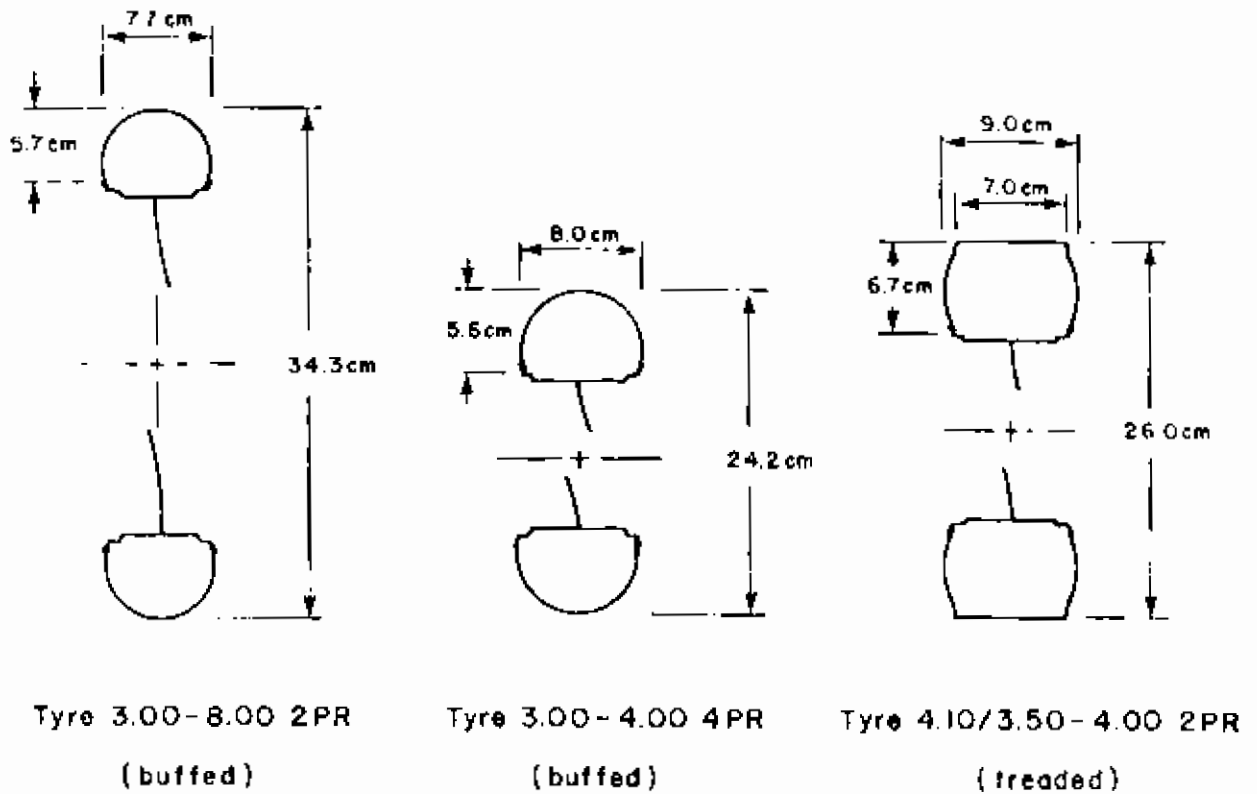
It is noted that if a rational method of analysis is to be developed for prediction of mobility performance characteristics of flexible wheels, it is evident that a proper accounting of tyre contribution is indeed necessary. In the application of the FEM technique, a method for application of the mechanics of energy transfer becomes available [see Yong et al., (1978)]. In the application of the principle involving energetics, there is a requirement for knowledge of the energy dissipation and transfer characteristics of tyres. These energy dissipation and transfer characteristics of tyres are seen to be conditioned

by the properties of the terrain [or reacting material] and by the stiffness properties of the tyres, the inflation pressures used and the type or properties of the surfaces of the tyres.

In this study, three candidate model tyres have been tested to determine properties relating to carcass stiffness and contact area development on rigid pavement, and soft soils. The information obtained allows for interpretation in terms of energy absorbing mechanisms. The contact areas developed for the tyres examined are evaluated with respect to the carcass stiffnesses of the tyres. The resultant contact pressures obtained are described accordingly to allow for their prescription as input to the prediction model - with solution sought through application of the FEM of analysis developed for loaded tyres and reported separately by Yong et al. (1978).

TYRE CHARACTERISTICS AND EXPERIMENTAL PROGRAM

Three model tyres were used in this study, namely Tyre 3.00-4.00 4PR [buffed], Tyre 3.00-8.00 2PR [buffed] and Tyre 4.10/3.50-4.00 2PR [treaded]. The dimensions of the undeformed sections for these tyres are shown in Fig. 1 together with their corresponding foot print patterns as determined from loading on to an unyielding surface. It is observed that the geometry of the contact areas of the buffed tyres are elliptical while that of the treaded tyre is approximately rectangular with two parallel and two slightly curved sides. Because of the size limitations of the tow bin, it was necessary to perform the tyre study on model tyres instead of on actual larger prototype tyres such as those used on the larger sized automobiles and farm vehicles. These candidate model tyres



Foot print pattern

Fig. 1 Undeformed Tyre Sections and Foot Print Patterns

were selected to study the influences of carcass stiffness, carcass shape, wheel diameter and inflation pressure.

The laboratory experiments performed were designed to produce the following information:

1. tyre load-deformation-inflation pressure relationships,
2. stationary tyre-rigid floor contact areas,
3. tyre-rigid floor contact areas under different slip rates,
4. stationary tyre-soil contact areas, and
5. mobility performances of tyres in the soil bin.

The details of test techniques and results obtained will be discussed in the succeeding sections. The finite element method of analysis which was developed to predict the tyre performances as a function of tyre properties and loading conditions is being presented separately [Yong et al., (1978)].

LOAD-DEFORMATION CHARACTERISTICS

In studying the load deformation characteristics of the tyres, the procedure of loading the stationary tyre through its rim whilst resting on an unyielding support was used. The response obtained is in terms of an increase in both deformation and contact area of the loaded tyre. To measure the contact area, the test tyre can be painted prior to loading, following which the imprinted foot print obtained after tyre loading can be measured. Alternatively, the test tyre can be placed on a thick plexi-glass and a photograph of the contact area obtained in the course of tyre loading. The latter technique provides one with the advantages of continuous measurements during increasing tyre loads and in

addition, a higher degree of accuracy can be achieved. Figure 2 shows a schematic view of the loading system and test measurement technique.

The loading test results for the three model tyres on a rigid unyielding surface of different inflation pressures shown in Fig. 3 demonstrate that tyre deformations increase linearly with axial loads. In addition, the results show that higher inflation pressures clearly improve tyre stiffness - as would be intuitively deduced. In practice, the inflation pressure is adjusted to match the applied wheel load so that tyre deflection is kept within workable limits. Comparing Tyre 3.00-8.00 2PR [buffed] and Tyre 3.00-4.00 4PR [buffed], it is observed that the former with 2-ply ratings exhibits less stiffness than the latter with a 4-ply ratings in the low inflation pressure ranges [0.07 and 0.21 ksc]. However, when the inflation pressure is increased, e.g. 0.41 ksc and 0.82 ksc, the result is reversed, i.e. the 2-ply tyre appears to be more stiff. The inflation pressure is thus seen to influence the load-resistance behaviour in addition to the tyre carcass structure and initial stiffness. The highest load-resistance capability exhibited by Tyre 4.10/3.50-4.00 2PR [treaded] is due mainly to the carcass construction which stiffened the carcass side walls with its treads.

CARCASS STIFFNESS

By assuming a uniform ground contact pressure distribution throughout the tyre-rigid surface contact area, the resultant ground pressure can be determined for the corresponding axial load and inflation pressure as shown in Fig. 4. For the buffed tyres, the tyre casings actually contact the ground in the loaded region. Thus the ground pressure will be equal to

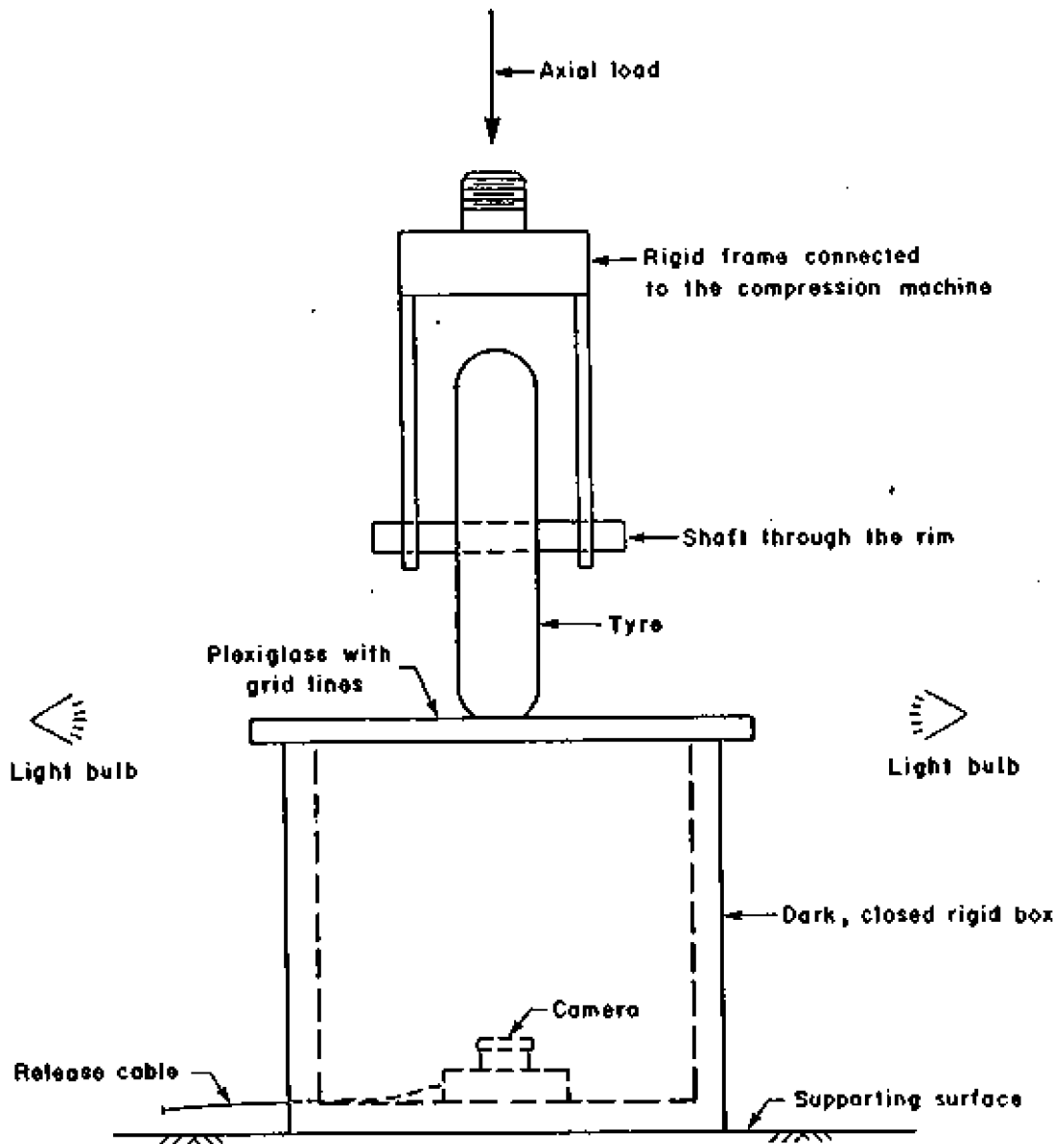


Fig. 2 Schematic View of Loading System and Test Measurement Technique

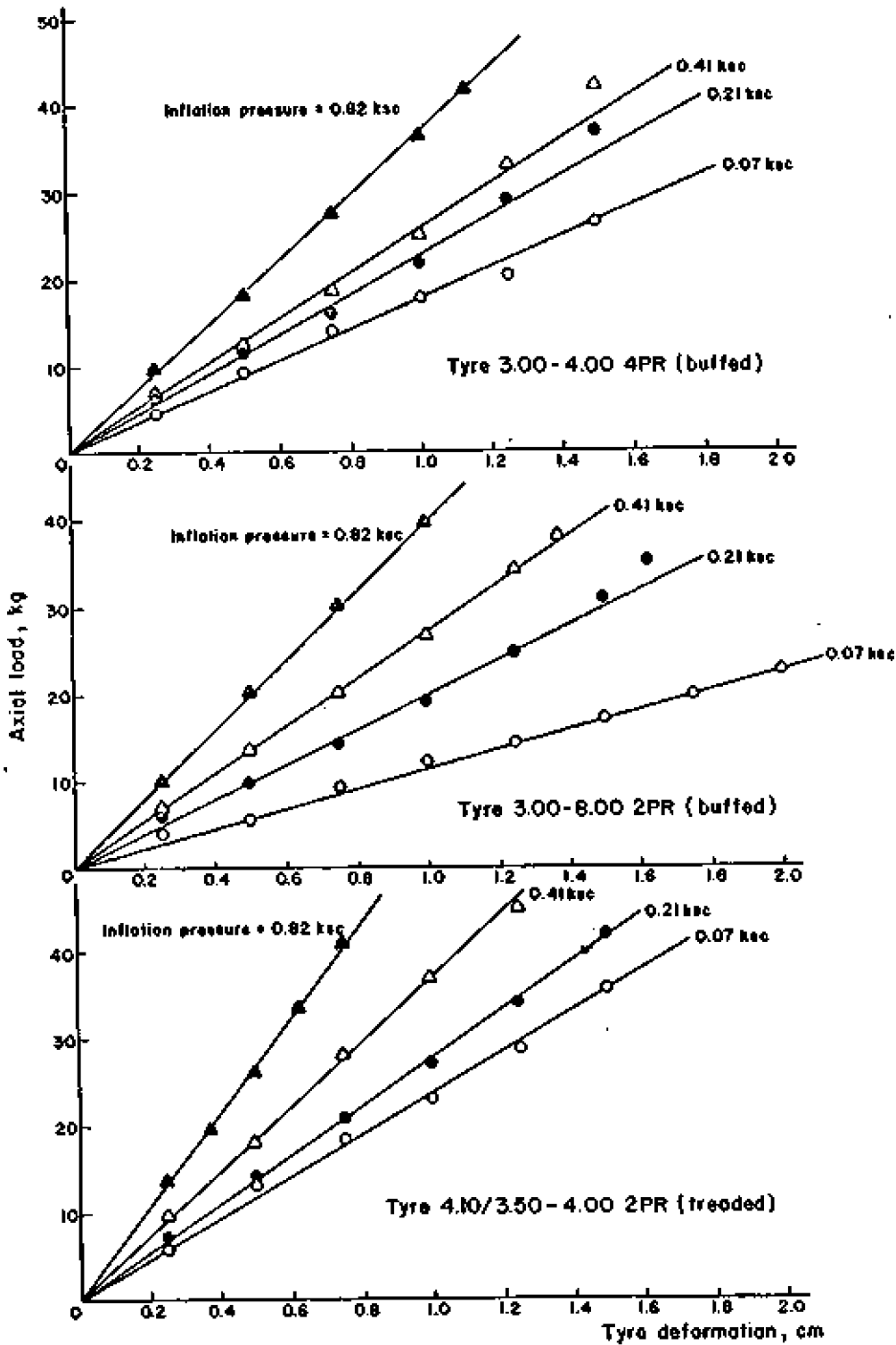


Fig. 3 Load-Deformation Characteristics

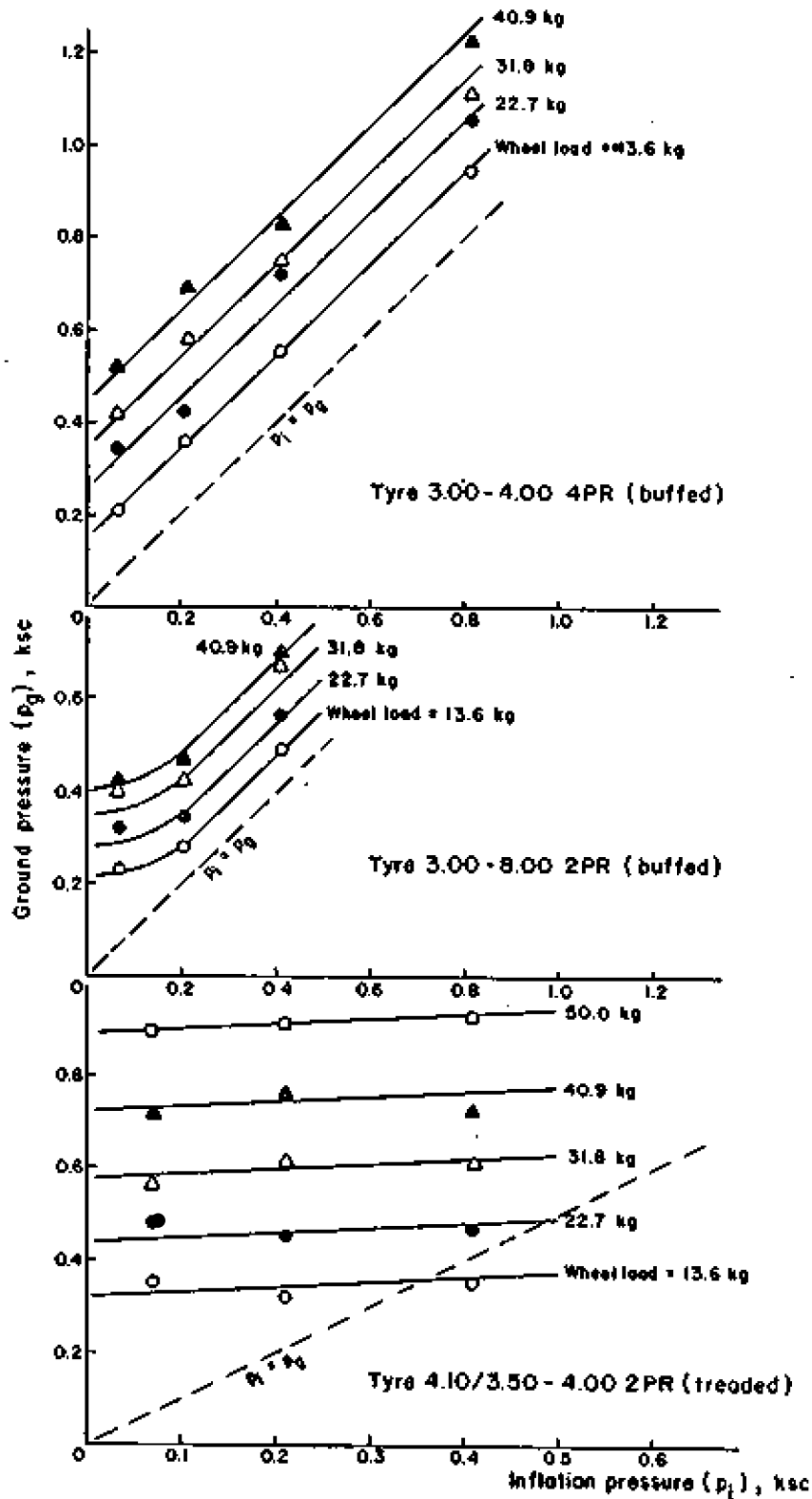


Fig. 4 Relationship of Ground Contact Pressure and Inflation Pressure

the inflation pressure used, with some extra pressure exerted by the tyre carcass at the transition zone between the casing side walls and the contact area [Clark, (1971)]. In the case of treaded tyres, it is evident that such a tyre will transmit the applied load from the hub to the ground through the actual contact between tyre tread and ground, thus creating the situation where the contact pressure is locally higher than the inflation pressure. The two buffed tyres clearly show the ground pressures to be always higher than the inflation pressures, while the treaded tyre sometimes shows the ground pressures to be less than the inflation pressures. This phenomenon can be attributed partly to the high carcass stiffness and partly to the gross contact areas used in the evaluation.

Defining the ground pressure p_g [Bekker and Semonin, (1975)] to be the sum of the inflation pressure p_i , and the carcass stiffness pressure p_c as :

$$p_g = p_i + p_c \quad (1)$$

it is observed in Fig. 4 that if the inflation pressure is kept constant, the carcass stiffness pressure p_c increases as the applied wheel load increases. Both the buffed tyres exhibit the same characteristic, i.e. the carcass stiffness pressures p_c are constant at the same wheel loads except in the low inflation pressures for Tyre 3.00-8.00 2PR [buffed] where the carcass stiffness pressures p_c are slightly higher than those in the high inflation pressure ranges. Unlike the other tyres, Tyre 4.10/3.50-4.00 2PR [treaded] shows the carcass stiffness pressure to decrease as the inflation pressure increases. Comparing all these model tyres under the same conditions, the degree of carcass stiffness can be classified

from the highest stiffness to the lowest as follows :

Tyre 4.10/3.50-4.00 2PR [treaded],

Tyre 3.00-4.00 4PR [buffed],

Tyre 3.00-8.00 2PR [buffed].

TYRE-RIGID SURFACE CONTACT AREAS AND SLIP RATES

In implementing the finite element method to analyze wheel-soil performance, such as that given by Yong et al., (1978), the contact area at the tyre-soil interface is an essential input to define the loaded boundary at the soil surface. Whilst it is difficult to measure the actual tyre-soil contact areas at various slip rates, it is possible to study the slip rate influence on the contact areas of the model tyres on an unyielding rigid surface. The test facilities employed herein have been presented earlier [Yong and Windisch, (1970)].

For this aspect of the study, the model tyres were controlled to move at a constant translational velocity of 15.2 cm/sec on a rigid floor made of plywood and partly of a thick 30 cm long plexi-glass. A 35-mm SLR camera was placed underneath the plexi-glass at a suitable distance and photographs of the resultant tyre contact areas moving over the plexi-glass were taken. The illumination system was adjusted to give clear contrast between the loaded and unloaded regions. The model tyres were subjected to two wheel loads [13.6 and 22.7 kg] and three inflation pressures [0.07, 0.21 and 0.41 ksc], each of which was tested from towed condition [approximately 0% slip] to 80% slip. From these tests, applied torques and developed drawbar pulls were also recorded.

The contact areas measured in this manner shown in Fig. 5 reveal that the contact areas between the tyres and the rigid surface are approximately constant at various slip rates. The contact areas measured statically are, in general, slightly higher than those measured under kinematic conditions. Both the buffed tyres show their contact areas to increase when wheel loads and inflation pressures are increased. For the treaded tyre, although the contact areas increase with wheel loads, they do not change significantly with inflation pressures. The behaviour is consistent with the results from stationary tests [Fig. 4].

ELASTIC MODULUS OF TYRE

The main factors which are seen to control the behaviour of a moving tyre are carcass stiffness, wheel load, inflation pressure, tyre casing dimensions and reacting terrain features. Leaving aside the terrain features, the theoretical approach that needs to be developed in order to predict tyre-soil contact area taking into account the governing factors, might begin with the Hertz theory of contact between two elastic bodies [Hertz, (1881)]. Following from this, the solutions for two cylindrical bodies in contact formulated by Poritsky (1950), might be obtained as :

$$\frac{1}{R_1} + \frac{1}{R_2} = \frac{4P}{\pi a^2} \left(\frac{1-\nu_1^2}{E_1} + \frac{1-\nu_2^2}{E_2} \right) \quad (2)$$

where

- R_1, R_2 = radius of the cylinder,
- P = applied vertical load,
- a = half length of the contact area,

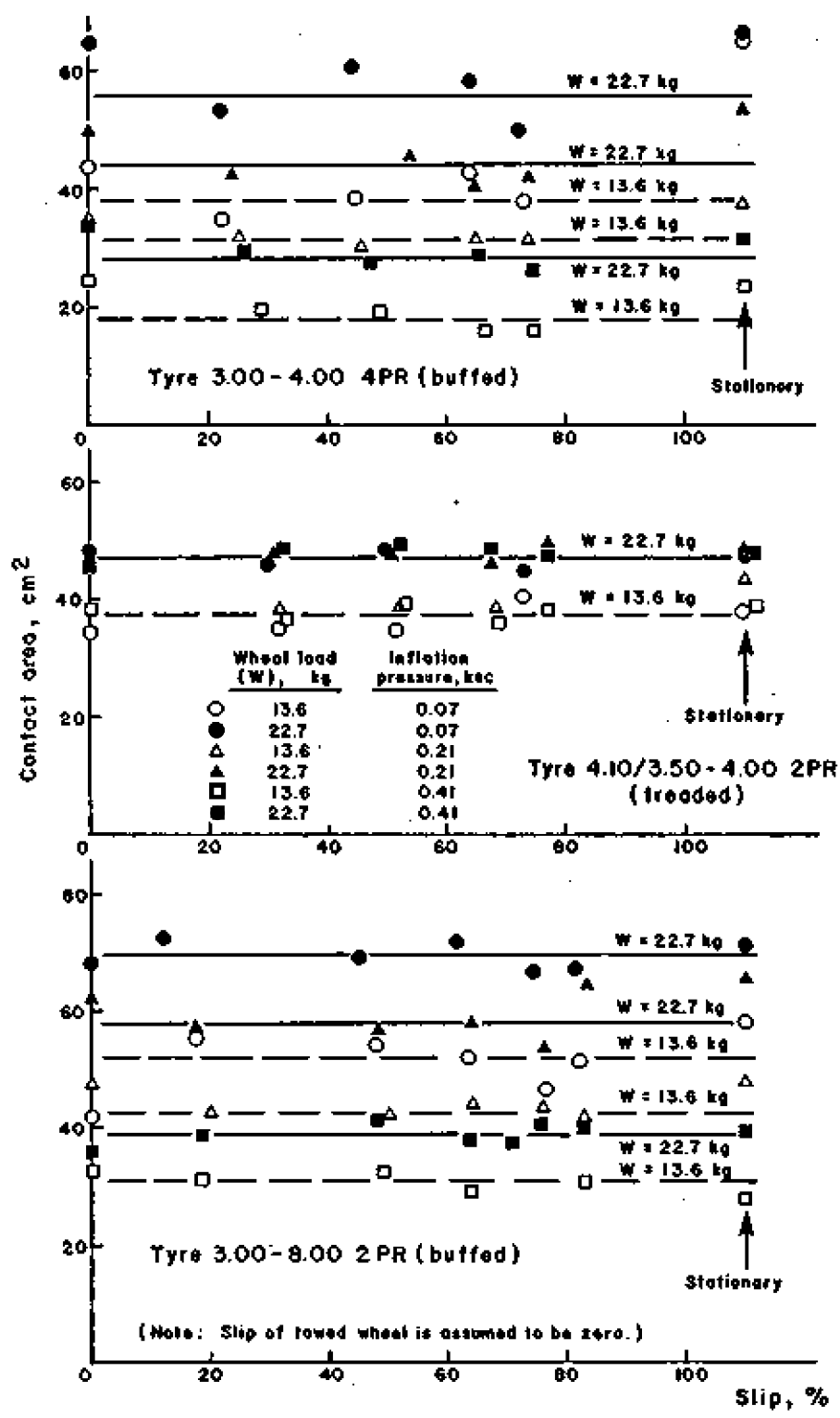


Fig. 5 Relationship of Tyre-Rigid Surface Contact Area and Slip Rates

ν_1, ν_2 = Poisson's ratio, and

E_1, E_2 = modulus of elasticity of the cylinder.

To adopt the Hertz contact theory for tyre-soil problems, the tyre may be idealized to be a cylinder of radius R_1 [Fig. 6] and the soil to be cylinder of infinite radius [$R_2 = \infty$]. This idealization is consistent with the two-dimensional requirements for input and application to the finite element method of analysis used by Yong et al, (1978). The contact area of the tyre-soil interface is thus approximated to be rectangular of length $2a$.

With a knowledge of tyre contact areas on rigid floor under stationary states, it is possible to evaluate the modulus of elasticity of the tyre E_1 which can be used to predict the tyre-soil contact areas. At small tyre deformation, the volume change of the tyre subjected to external loading is relatively small so that the Poisson's ratio ν_1 may be taken as 0.5. The modulus of elasticity of the rigid floor can be assumed to be infinite from which the last term of Eq. (2) becomes zero. It should be noted at this stage that the elastic modulus of the tyre E_1 refers not only to the tyre itself but also reflects the characteristic of the whole tyre system, i.e. tyre carcass stiffness, inflation pressure and hub.

The results obtained [Fig. 7] show that the elastic modulus of the tyre E_1 increases linearly with the inflation pressure. Each of the buffed tyres tends to follow a single linear relationship between the elastic modulus and the inflation pressure, while the elastic modulus of Tyre 4.10/3.50-4.00 2PR [treaded] increases as both wheel load and inflation pressure increases.

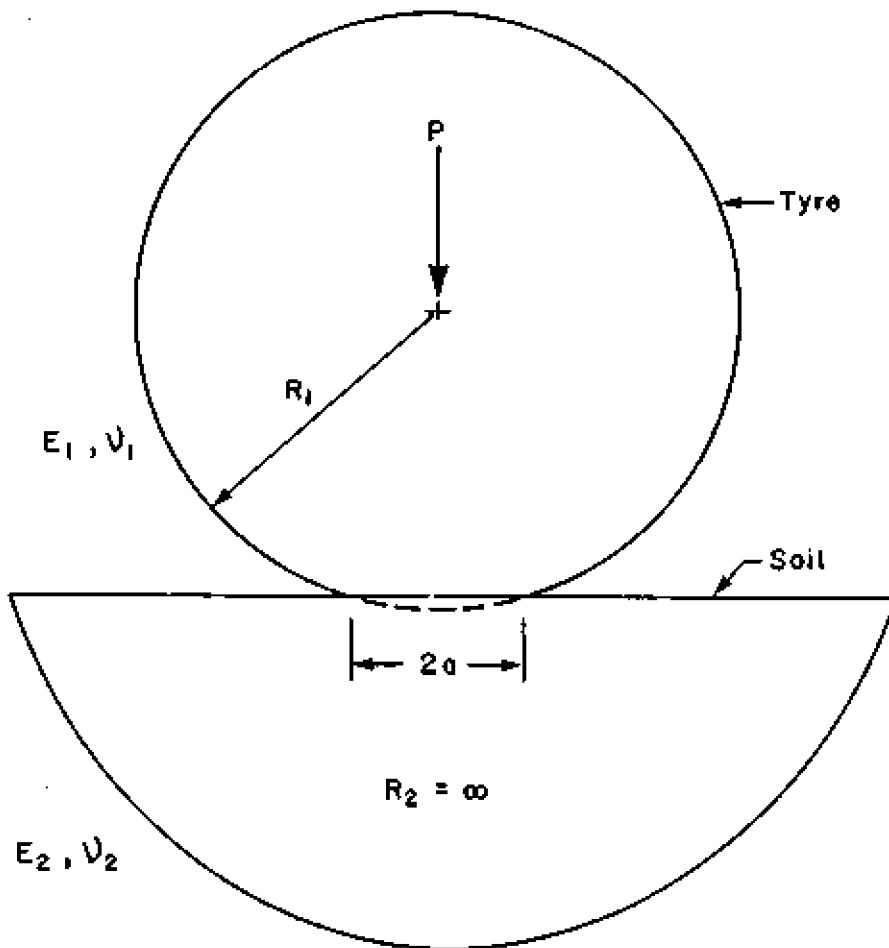


Fig. 6 Idealization of Tyre and Soil in Contact

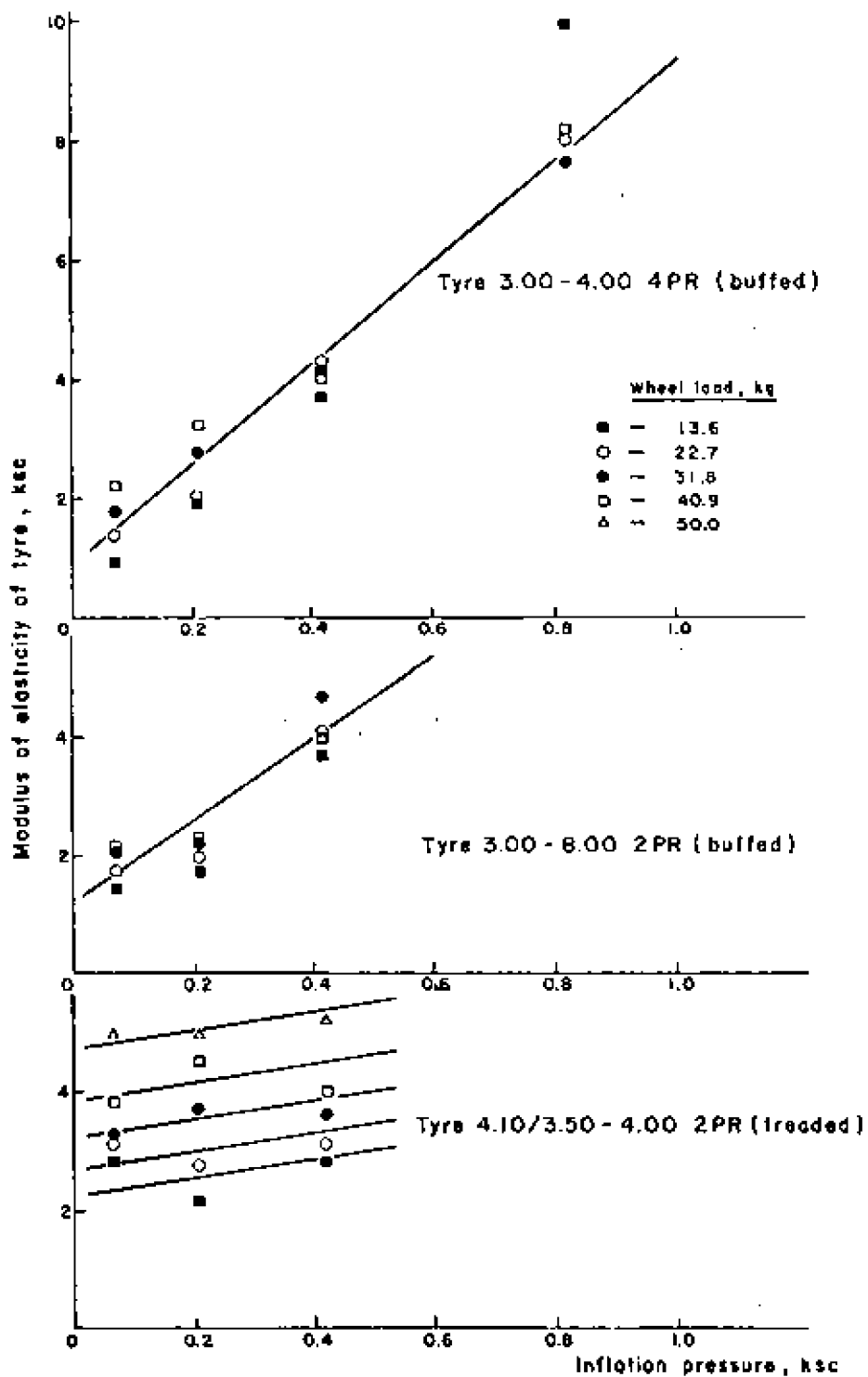


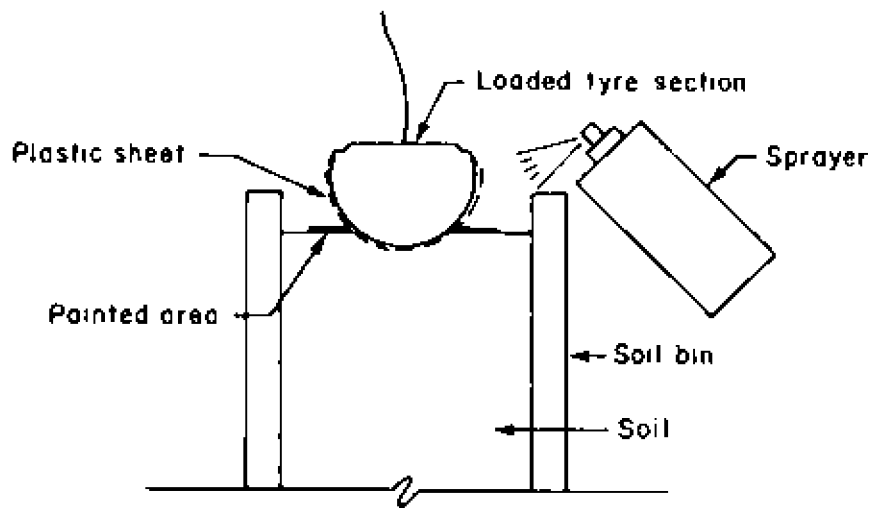
Fig. 7 Modulus of Elasticity of Tyre .

PREDICTION OF TYRE-SOIL CONTACT AREAS

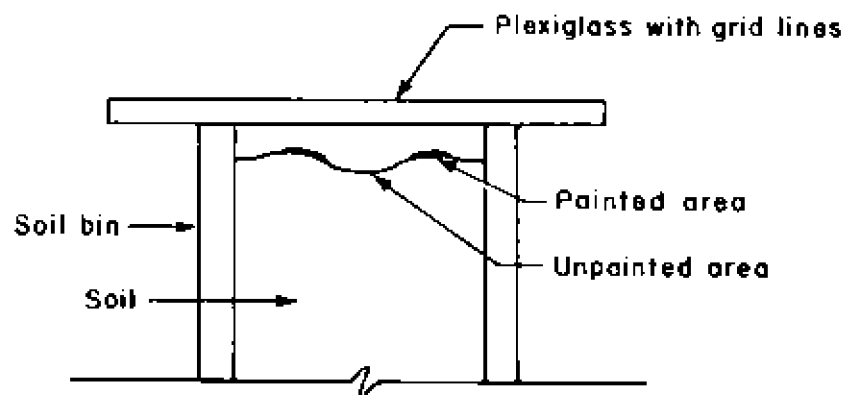
In order to validate the capability for predicting tyre-soil contact areas, the model tyres were tested on two different soils, i.e. kaolinite clay and silty soil. The technique used for measuring tyre-soil contact areas is shown schematically in Fig. 8. This procedure was adopted to provide a means to distinguish, as clearly as possible, the actual contact areas. Prior to placing the tyre on the soil, the tyre was covered with a piece of plastic sheet so that the soil would not stick to the tyre. Following spray painting, the tyre with the plastic sheet was carefully removed, leaving the clear contact area on the soil surface. A piece of plexi-glass with grid lines was then placed on top of the soil bin and a photograph was taken.

The stress-strain relationships of both soils shown in Figs. 9 and 10 were tested in plane strain conditions to duplicate the situation in the soil bin. The kaolinite clay was compacted with the moisture content of 42 to 44% producing thereby a degree of saturation of 95%. The silty soil was a mixture of fine sand [passing sieve No.30] and kaolinite at 30% of sand dry weight. The dry compacted density was 1.88 tons/m^3 at 13% moisture content throughout the test program.

The procedure for prediction of tyre-soil contact areas can be achieved by using Eq.(2) and the modulus of elasticity of the candidate tyres, E_1 [Fig. 7]. To apply this procedure, the modulus of elasticity of the silty soil E_2 was taken from the initial tangent modulus [32 ksc] at the low confining pressure since the wheel loads tested were relatively small with respect to the soil stiffness. In the case of the soft kaolinite clay, E_2 [0.75 ksc] was selected to be the secant modulus at



(a) Load the tyre on the soil



(b) Remove the tyre and take a photograph

Fig. 8 Procedure of Measuring Tyre-Soil Contact Area

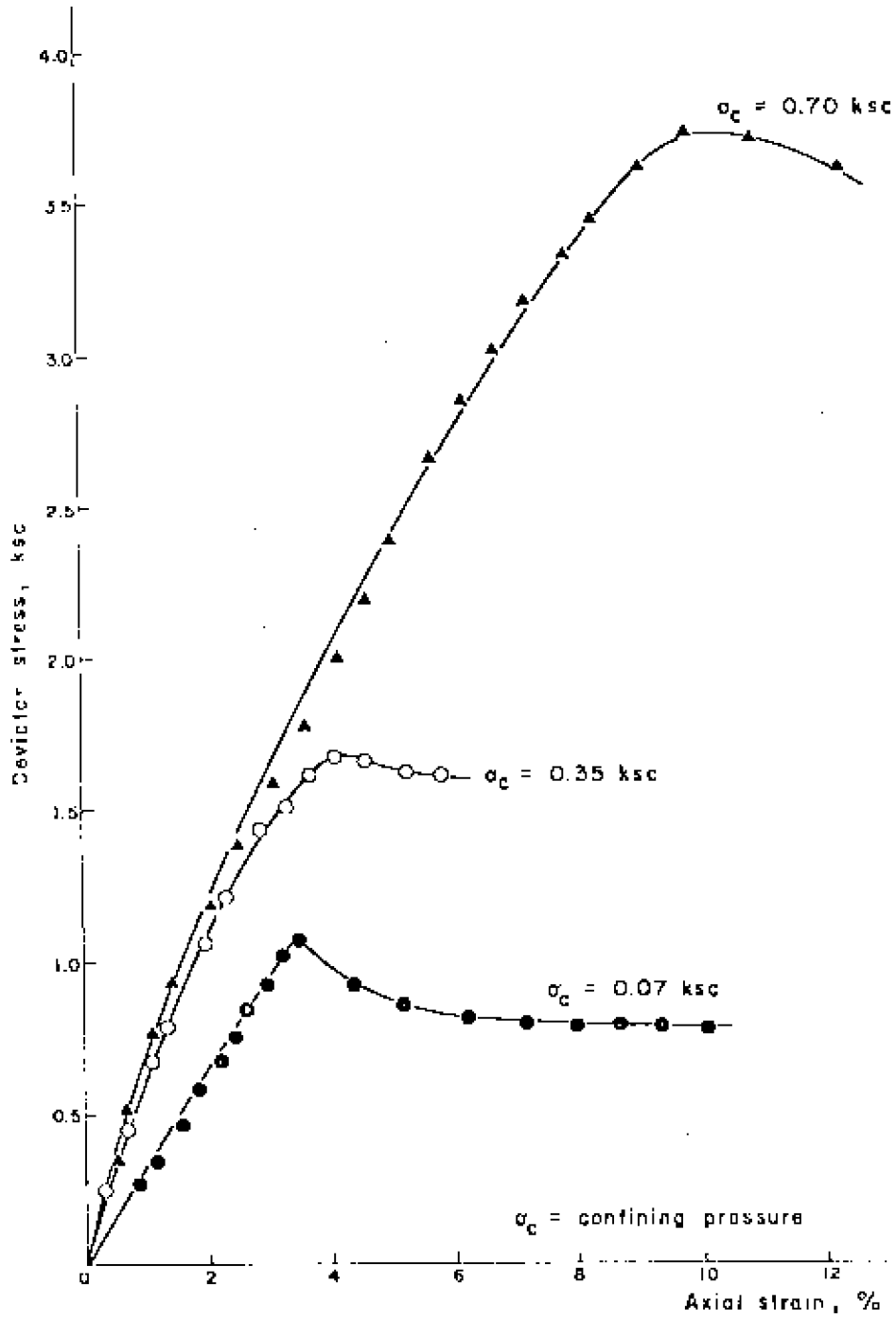


Fig. 9 Stress-Strain Relationship of Silty Soil under Plane-Strain Triaxial Test

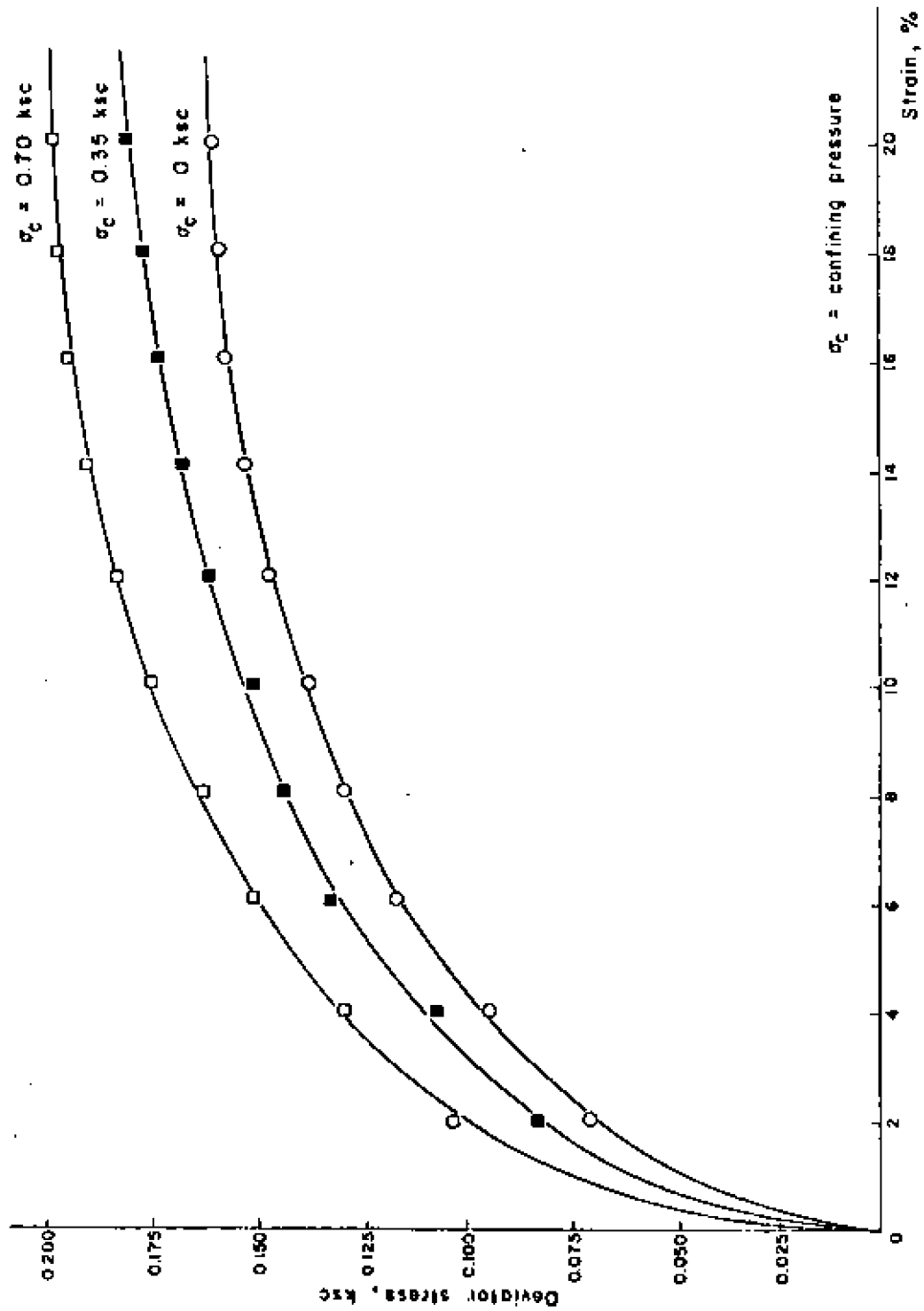


Fig. 10 Stress-Strain Curves of Kaolinite Clay under Plane-Strain Triaxial Tests

20% strain. This is justified since the wheel loads used were high compared to the strength of the clay. The Poisson's ratio of the soils was taken as 0.5 since they were almost fully saturated.

To implement the prediction procedure, it is necessary to begin with the determination of the width of the contact area. The flow chart given in Fig. 11 demonstrates the procedure to be followed. Since the change in the width of the contact area is not as rapid as the change in the length, the width may be assumed to be equal to that of the tyre-rigid surface contact area. With the knowledge of the ground pressure-inflation pressure relationship [Fig. 4], the tyre-rigid surface contact area can be evaluated. A trial and error procedure needs to be implemented to match the width and the length of the contact area predicted by using Eq. (2). In general, the contact width obtained will be slightly less than the measured one. Once the width of the contact area is known, the length can be predicted with the aid of Eq. (2) and the tyre-soil properties. In the case of Tyre 4.10/3.50-4.00 2PR [treaded], the width of the contact area was kept constant.

The results of the tyre-soil contact areas predicted by this procedure [Figs. 12 and 13] show good agreement in both soils. It is observed that the contact area increases linearly as the wheel load applied is increased and also increases as the inflation pressure used is decreased. The capability of the proposed approach to predict the tyre-soil contact areas with respect to the changes in wheel load, inflation pressure and soil type is clearly demonstrated.

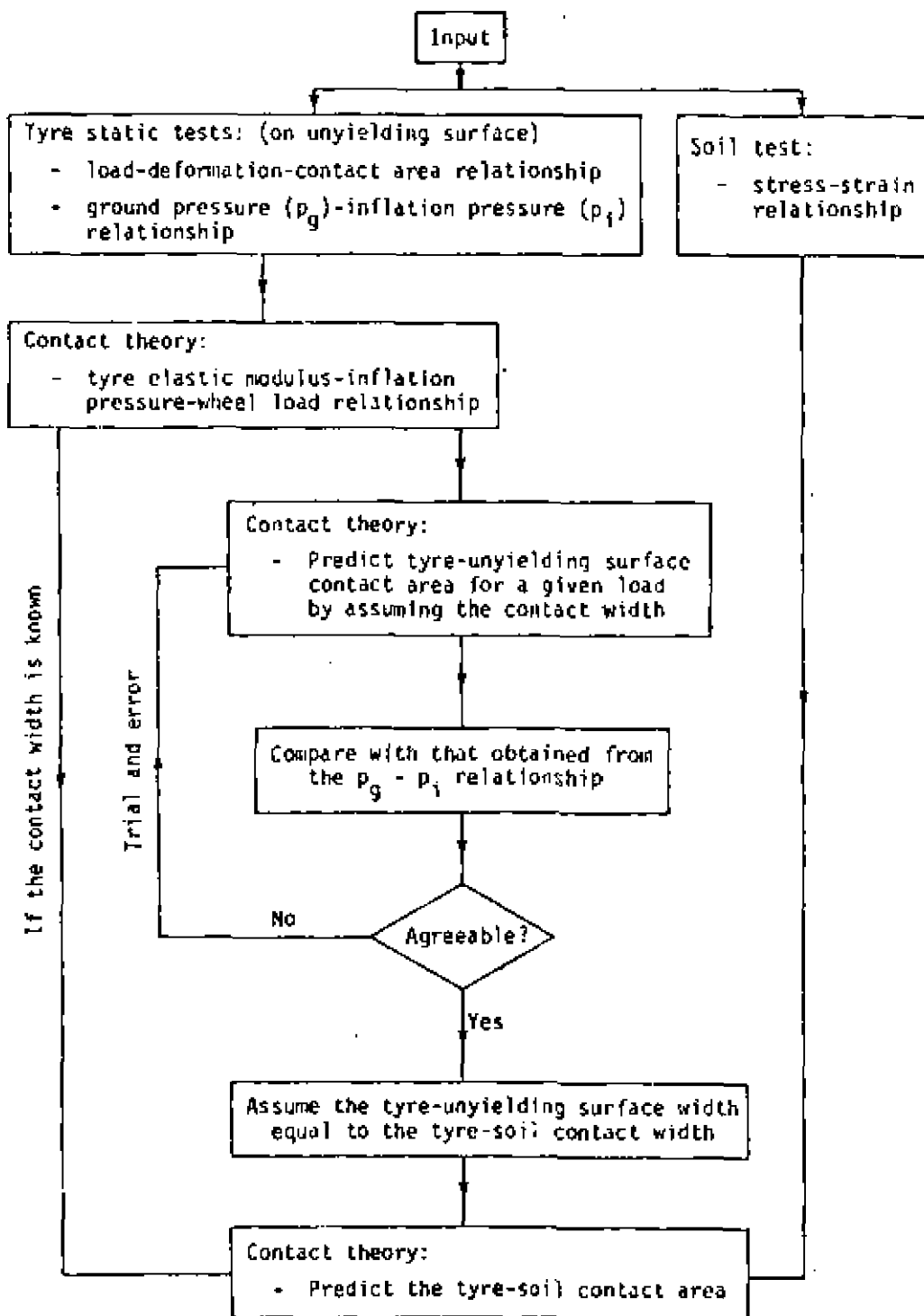


Fig. 11 Flow Chart of Predicting Tyre-Soil Contact Area

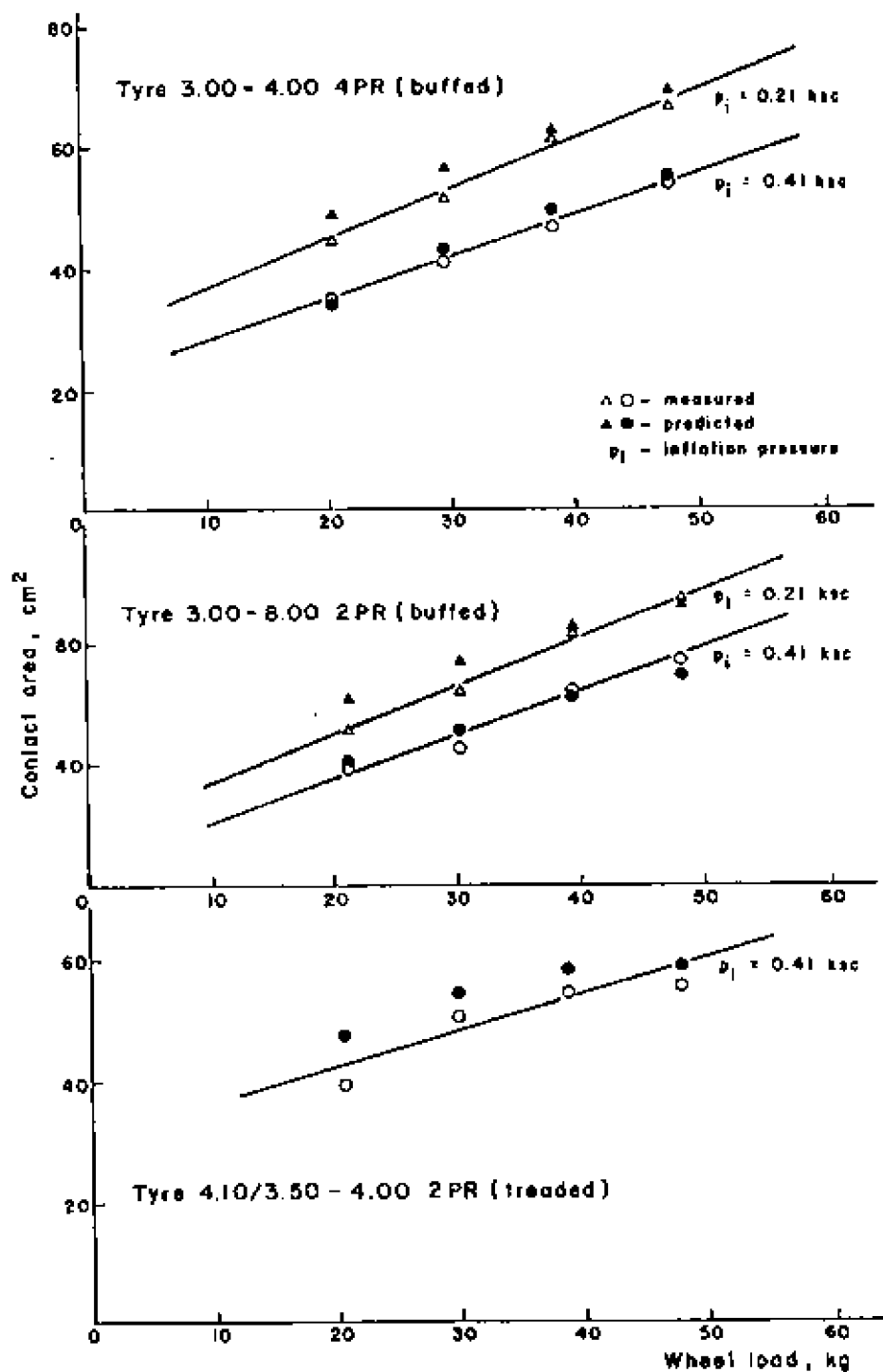


Fig. 12 Contact Areas of Tyres on Silty Soil

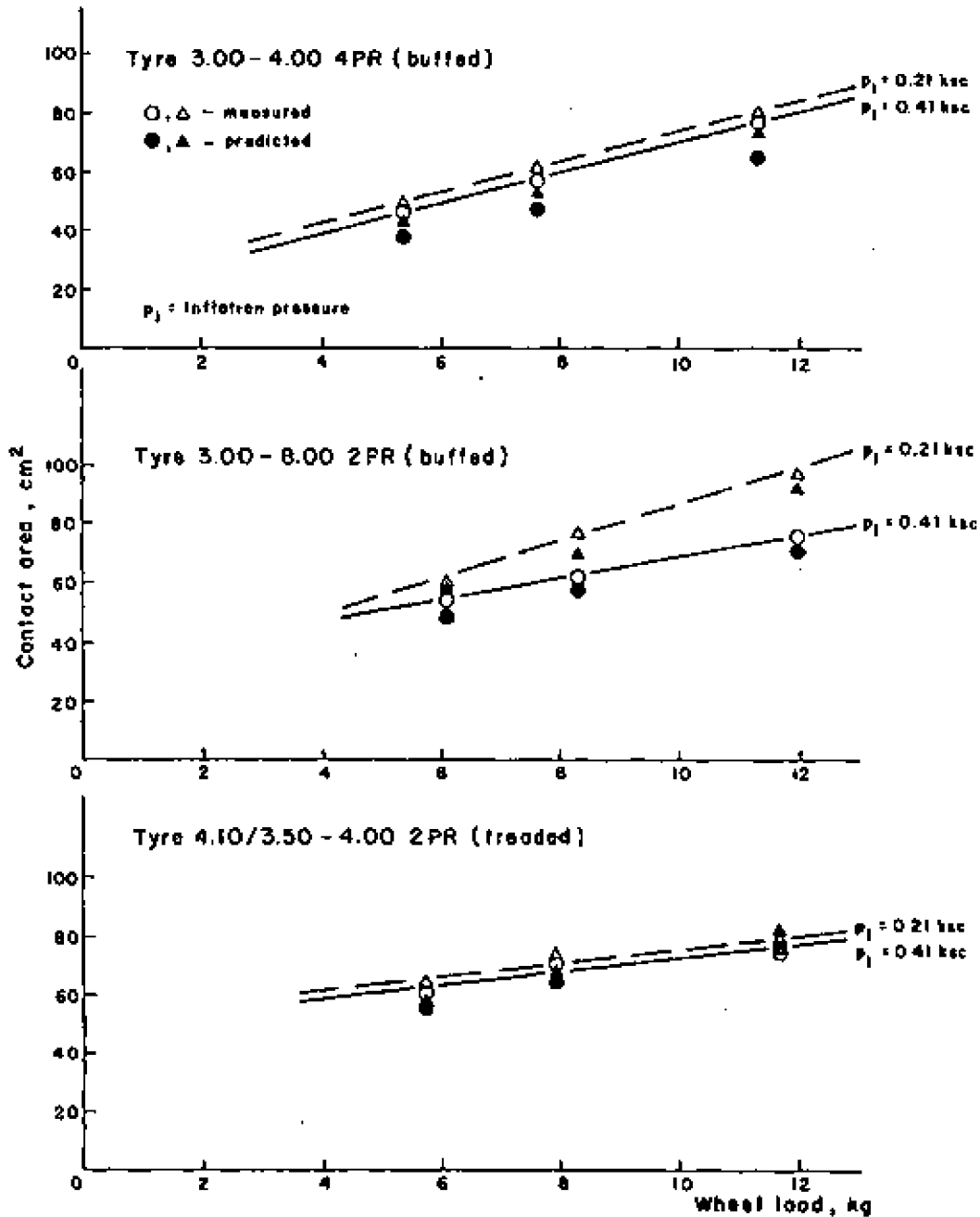


Fig. 13 Contact Areas of Model Tyres on Kaolinite Clay

CONCLUDING REMARKS -
PERFORMANCE OF THE MODEL TYRES ON UNYIELDING RIGID FLOOR

In applying the energy approach proposed by Yong and Webb (1969) to evaluate the rigid wheel-soil performance at any degree of slip, it is necessary to consider the energy expended in deforming the flexible pneumatic tyre. The interaction between moving tyre and soil can be written in terms of participating energies as :

$$E^I = D^I + P_o + E_f + E_t \quad (3)$$

where

E^I = input energy,

D^I = soil deformation energy,

P_o = useful output energy,

E_f = interfacial energy, and

E_t = tyre-deforming energy.

All the energy components are evaluated as the amount of energy developed for one unit width of the contact area and one unit of travel distance, i.e. kg-cm/cm/sec. In order to formulate an appropriate approach to predict the energy spent in deforming the tyre, it is necessary to investigate the characteristic of this particular energy component in detail. By moving the model tyres on a rigid floor and measuring the applied torques and drawbar pulls at various slip rates, the tyre-deforming energy can then be studied. Since the soil deformation energy D^I of the rigid surface is essentially zero, Eq. (3) can be rewritten as :

$$E_t = E^I - P_o - E_f \quad (4)$$

and with the measured torque T and drawbar pull P , the following expressions can be calculated :

$$\left. \begin{aligned} E' &= T\omega \\ P_o &= PV \\ E_f &= \frac{T}{r} (\omega r - V) \end{aligned} \right\} (5)$$

where

ω = rotational velocity rad/sec,

V = translational velocity cm/sec,

r = rolling radius of the tyre, cm.

The tyre-deforming energies obtained by this procedure at different wheel loads, inflation pressures and slip rates are presented in Fig. 14. All the model tyres tested show that the energies spent in deforming the tyres are insignificantly affected by the degrees of slip. This is attributed to the fact that the carcass stiffnesses of the tyres were large. It is expected that with less stiff tyres the influence of slip would be noticed. It is obvious that for this series of tests [on stiff tyres] the wheel load and the inflation pressure used are the major factors controlling the tyre-deforming energy [Fig. 15]. When the stiffness of the tyres is reduced, it is expected that a greater energy expenditure in tyre deformation can be obtained.

Alternatively, one may choose to use a predictive model solely for determination of the tyre deformation energy E_t . In such a case, the tyre deformation created by the normal pressure is calculated from the difference between the resultant soil displacement at the tyre-soil contact area obtained in the finite element method such as that used by

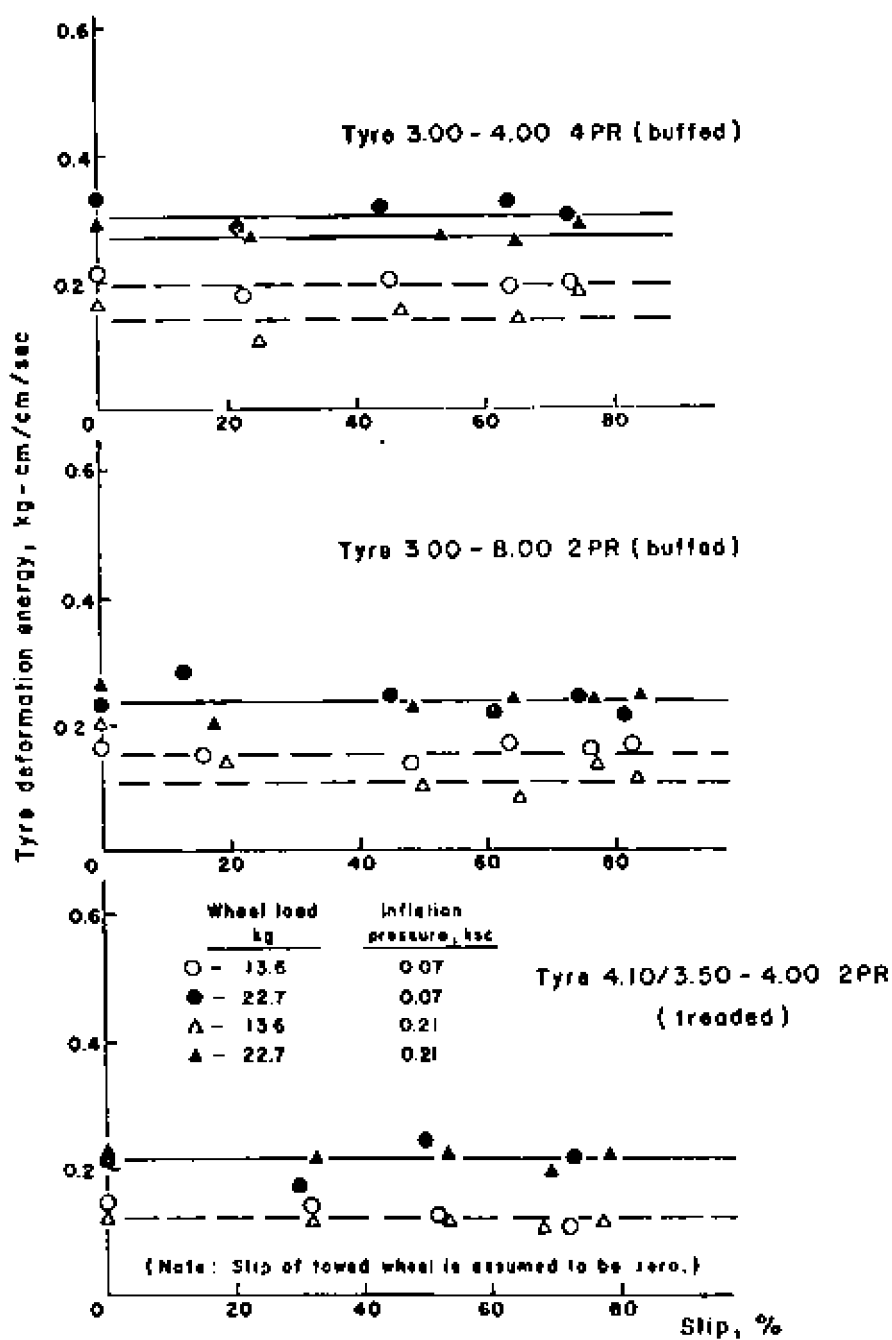


Fig. 14 Relationship of Measured Tyre-Deformation Energy and Slip Rate

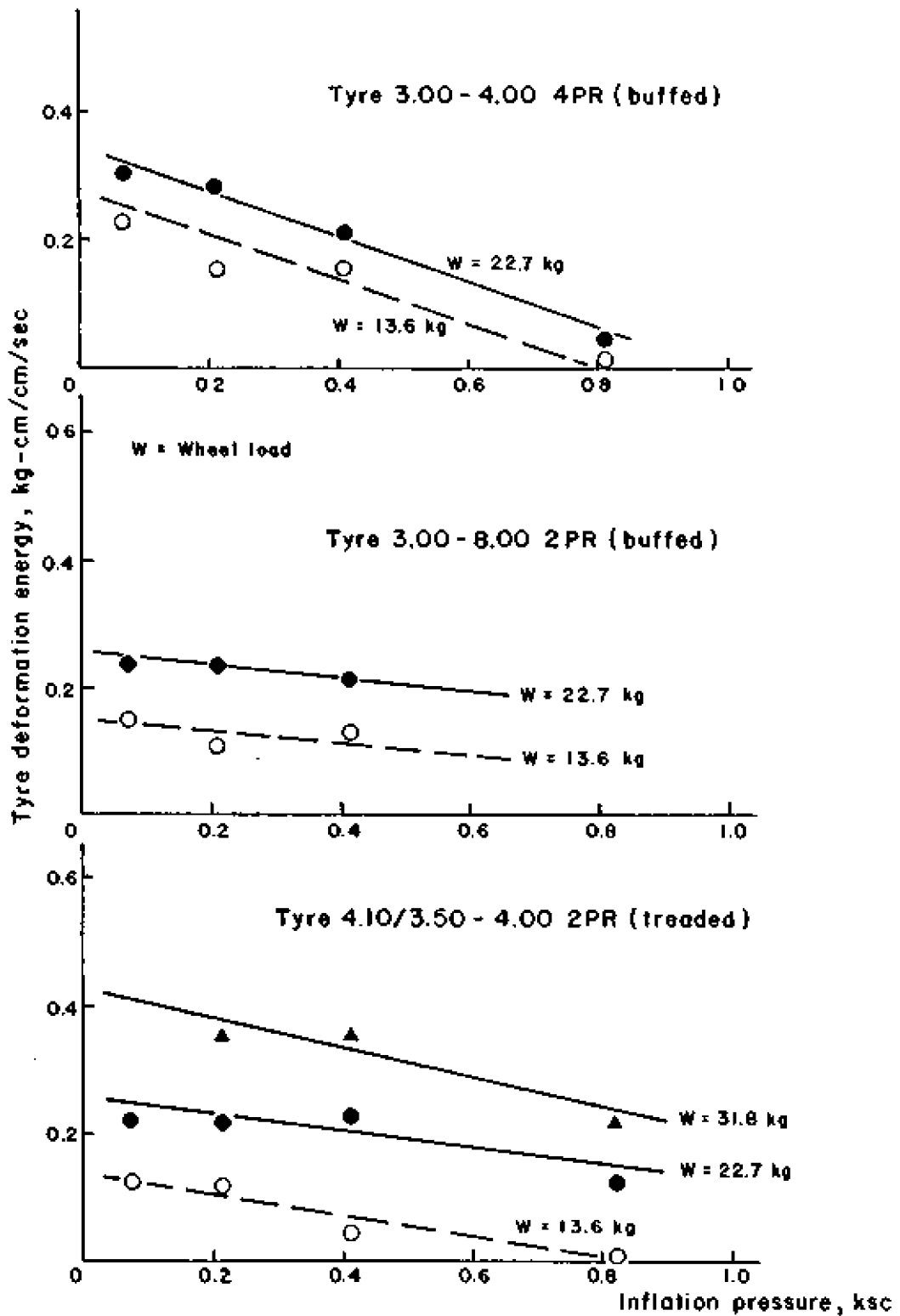


Fig. 15 Relationship of Tyre-Deformation Energy and Inflation Pressure

Yong and Fattah (1976) and Yong et al (1978), and the original undeformed tyre configuration [Fig. 16]. The first and last nodes [nodes 1 and 5] of the contact area are used as the reference datum for the fictitious undeformed surface of the tyre so that the tyre deformation δ at the loaded nodes can be evaluated i.e. [δ_2 , δ_3 and δ_4]. The tyre distortion due to tangential stresses is neglected since the tyre is moving at low speed. The total tyre deformation energy E_t can now be expressed as:

$$E_t = \frac{B \sum_{i=1}^n P_i \delta_i}{\alpha R} V \quad (6)$$

where

B = tyre width, cm,

P_i = nodal force at node i , kg,

δ_i = tyre deformation at node i , cm,

α = angle sustained by the contact area [Fig. 16], rad,

R = rolling radius, cm,

V = translational velocity, cm/sec.

The subsoil deformation energy per unit width can be calculated as:

$$D^1 = \iint \sigma \dot{\epsilon} dx dy \quad (7)$$

where

σ = stress acting on the finite element,

$\dot{\epsilon}$ = incremental strain rate,

$dx dy$ = dimension of the element.

The other energy components of Eq. (3), i.e. the input energy E^1 , the useful output energy P_o and the interfacial energy E_f , are determined

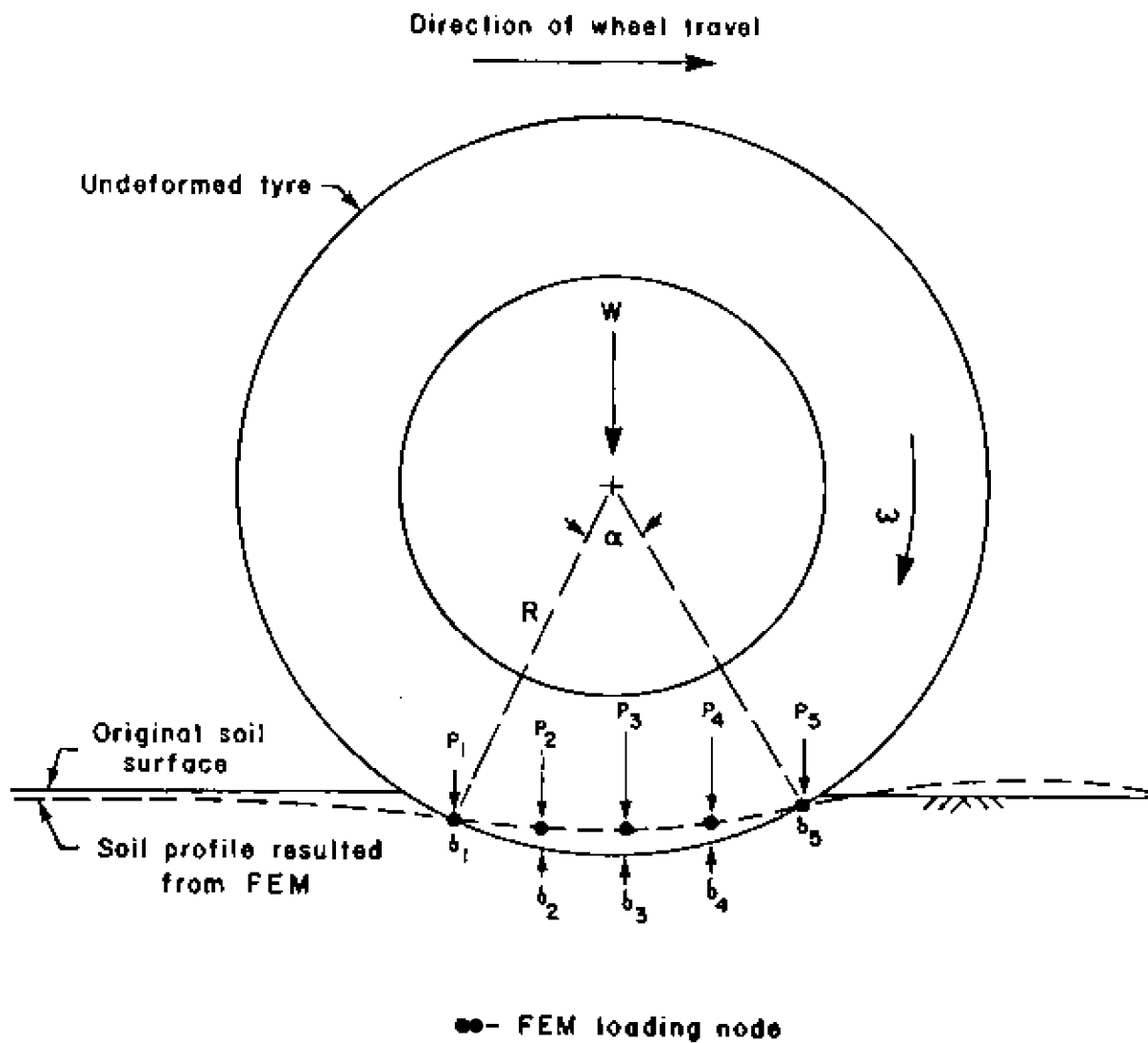


Fig. 16 Determination of Tyre Deformation Resistance

by using Eq. (5).

Yong, Fattah and Boonsinsuk (1978) have applied the FEM technique to the study of the performances of the model tyres on the silty soil. The measured torques were used as input data so that the input energy E^I and the interfacial energy E_f were known and the FEM was then carried out to evaluate the tyre deformation energy E_t and the soil deformation energy D^I . The useful output energy P_o was obtained by using Eq. (3) and compared with the measured value. The results of Tyre 3.00-4.00 4PR [buffed] moving on the silty soil with the wheel load of 31.8 kg and the inflation pressure of 0.82 ksc were analysed according to the above procedure and good agreement between the predicted and measured output energies is shown in Fig. 17.

ACKNOWLEDGEMENTS

This study was conducted under contract arrangement with the Department of Supply and Services - with project administration from the Mobility Section of Defence Research Establishment Ottawa (DREO). The assistance and input given by the Project Officer, Mr. I. S. Lindsay, Earth Sciences Division, are acknowledged.

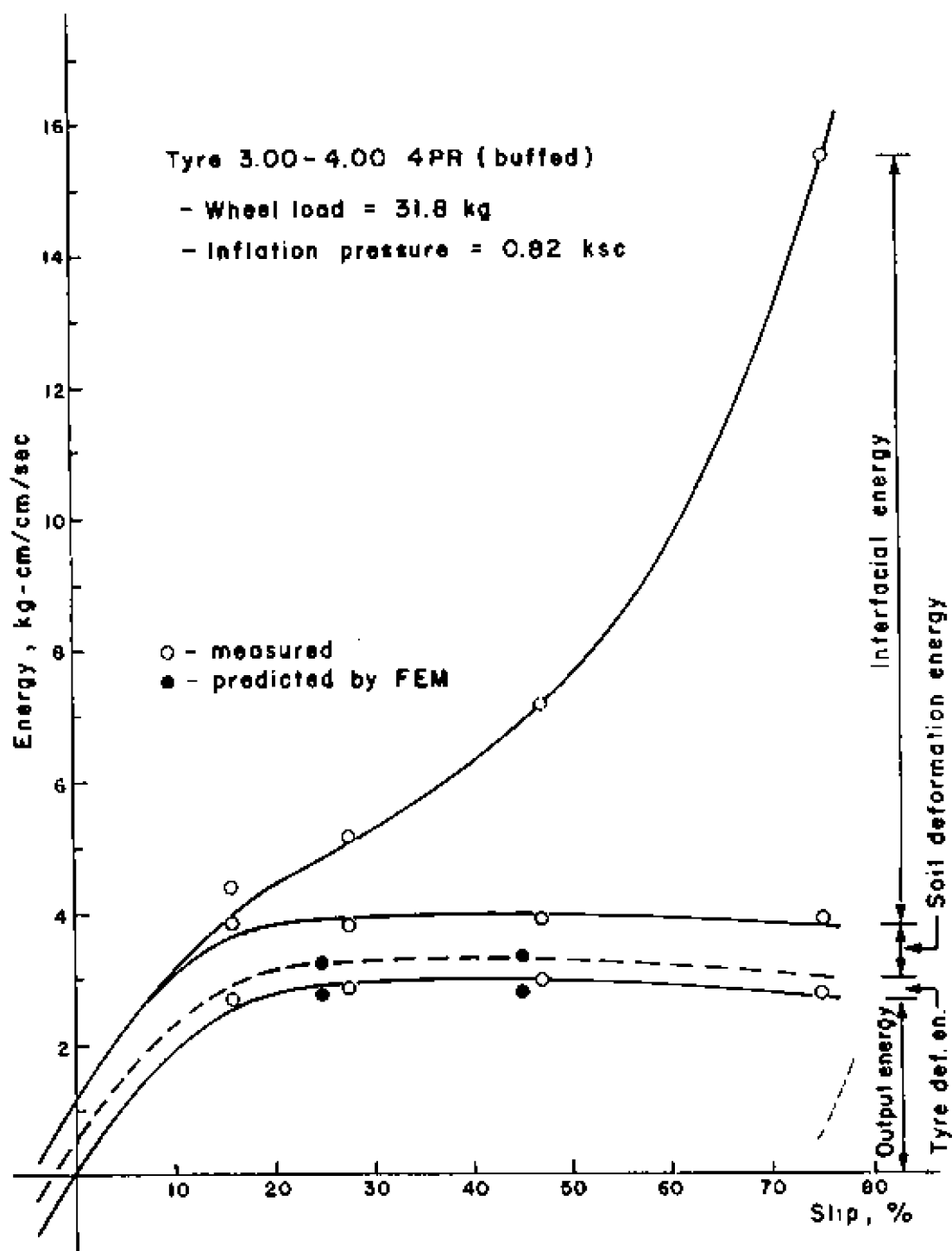


Fig. 17 Energy Balance of Tyre 3.00-4.00 4PR (Buffed) Moving on Silty Soil

REFERENCES

1. S. M. Clark, *MECHANICS OF PNEUMATIC TIRES*, University of Michigan, Ann Arbor, Michigan. (1971).
2. M. G. Bekker and E. V. Semonin, *Motion Resistance of Pneumatic Tyres*, *J. Automotive Engineering*, pp. 6-10. (1975).
3. R. N. Yong and E. Windisch, *Determination of Wheel Contact Stresses from Measured Instantaneous Soil Deformations*, *J. Terramechanics*, 7:57-67. (1970).
4. H. Poritsky, *Stresses and Deflections of Cylindrical Bodies in Contact with Application to Contact of Gears and of Locomotive Wheels*, *J. Applied Mech*, 17:191-201. (1950).
5. R. N. Yong and G. L. Webb, *Energy Dissipation and Drawbar Pull Prediction in Soil-Wheel Interaction*, *Proc., Third Int. Conf. ISTVS, Essen, Vol.1, 93-142. (1969).*
6. R. N. Yong and E. A. Fattah, *Prediction of Wheel-Soil Interaction and Performance using the Finite Element Method*, *J. Terramechanics* 13, 227-240. (1976).
7. D. R. Freitag, A. J. Green and N. R. Murphy, Jr., *Normal Stresses at the Tire-Soil Interface in Yielding Soils*, *Highway Research Record* 74, 1-18. (1964).
8. G. Krick, *Radial and Shear Stress Distribution under Rigid Wheels and Pneumatic Tyres operating on Yielding Soils with consideration of Tire Deformation*, *J. Terramechanics* 6:3, 73-98. (1969).
9. R. N. Yong, E. A. Fattah and P. Boonsinsuk, *Analysis and Prediction of Tyre-Soil Interaction and Performance using Finite Elements*, *J. Terramechanics (In Press) 1978.*